การหาค่าแรงโก่งเดาะโดยใช้ฟังก์ชั่นรูปร่างที่ปรับได้

นาย นิจวิชัย วัชรากร

วิทยานิพนธ์นี้เป็นส่วนหนึ่งของการศึกษาตามหลักสูตรปริญญาวิศวกรรมศาสตรมหาบัณฑิต
สาขาวิชาวิศวกรรมโยธา   ภาควิชาวิศวกรรมโยธา
คณะวิศวกรรมศาสตร์ จุฬาลงกรณ์มหาวิทยาลัย
ปีการศึกษา 2553

DETERMINATION OF BUCKLING LOAD BY ADAPTIVE SHAPE FUNCTIONS

Mr. Nidvichai Watcharakorn

A Thesis Submitted in Partial Fulfillment of the Requirements

for the Degree of Master of Engineering Program in Civil Engineering

Department of Civil Engineering

Faculty of Engineering

Chulalongkorn University

Academic Year 2010

Thesis Title   DETERMINATION OF BUCKLING LOAD BY ADAPTIVE SHAPE

                      FUNCTIONS

By   Mr. Nidvichai Watcharakorn

Field of Study   Civil Engineering

Thesis Advisor   Assistant Professor Jaroon Rungamornrat, Ph. D.

Accepted by the Faculty of Engineering, Chulalongkorn University in Partial

Fulfillment of the Requirements for the Master's Degree

.... Dean of the Faculty of Engineering

(Associate Professor Boonsom Lerdhirunwong, Dr.Ing.)

THESIS COMMITTEE

.... Chairman

(Professor Teerapong Senjuntichai, Ph.D.)

.... Thesis Advisor

(Assistant Professor Jaroon Rungamornrat, Ph.D.)

.... Examiner

(Assistant Professor Watanachai Smittakorn, Ph.D.)

.... External Examiner

(Associate Professor Pruettha Nanakorn, D.Eng.)

นิจวิชัย   วัชรากร   :   การหาค่าแรงโก่งเดาะโดยใช้ฟังก์ชั่นรูปร่างที่ปรับได้. (DETERMINATION OF BUCKLING LOAD BY ADAPTIVE SHAPE FUNCTIONS) อ. ที่ปรึกษาวิทยานิพนธ์หลัก: ผศ.ดร. จรูญ รุ่งอมรรัตน์, 67 หน้า.

การศึกษาในวิทยานิพนธ์ฉบับนี้นำเสนอการพัฒนาระเบียบวิธีเชิงตัวเลขที่ถูกต้องและมีประสิทธิภาพสำหรับคำนวณค่าแรงโก่งเดาะของโครงสร้าง 2 มิติ สมการกำกับสร้างโดยอาศัยหลักการพลังงานศักย์รวมคงที่ และคำตอบเชิงตัวเลขคำนวณจากหลักการประมาณของเรย์เล-ริตซ์ จุดเด่นที่สำคัญของระเบียบวิธีที่พัฒนาขึ้นคือเซตของฟังก์ชันที่ใช้ในการประมาณรูปร่างการโก่งเดาะสร้างมาจากฟังก์ชันรูปร่างที่มีพารามิเตอร์ซึ่งสามารถปรับเปลี่ยนค่าได้อยู่ด้วย โดยที่พารามิเตอร์ดังกล่าวมีความสัมพันธ์โดยตรงกับค่าแรงอัดตามแนวแกนของชิ้นส่วน และที่สำคัญคือเซตดังกล่าวนี้จะมีรูปร่างการโก่งเดาะแม่นตรงเป็นสมาชิกด้วย เมื่อแรงอัดตามแนวแกนมีค่าเท่ากับแรงโก่งเดาะของชิ้นส่วน   ฟังก์ชันฐานแบบพิเศษนี้สร้างขึ้นจากผลเฉลยแม่นตรงของสมการเชิงอนุพันธ์ที่กำกับพฤติกรรมการโก่งเดาะของชิ้นส่วน   โดยพิจารณาชิ้นส่วนหลายประเภท อาทิเช่น ชิ้นส่วนทั้งที่มีและไม่มีค้ำยันด้านข้าง ชิ้นส่วนที่พิจารณาผลของการเปลี่ยนรูปเนื่องจากแรงเฉือน   และชิ้นส่วนที่ทำมาจากวัสดุไม่ยืดหยุ่น   ชิ้นส่วนที่พิจารณาผลต่างๆเหล่านี้ช่วยเพิ่มความสามารถในการวิเคราะห์ค่าแรงโก่งเดาะของโครงสร้างได้หลากหลาย (อาทิเช่น โครงข้อแข็งทั้งที่มีและไม่มีค้ำยันด้านข้าง เสาที่วางอยู่บนฐานรากยืดหยุ่น เสาที่เกิดการโก่งเดาะในช่วงไม่ยืดหยุ่น และโครงสร้างที่ผลการเปลี่ยนรูปเนื่องจากแรงเฉือนมีนัยสำคัญ เป็นต้น) การใช้ฟังก์ชันประมาณที่ปรับได้ร่วมกับกระบวนการทำซ้ำที่เหมาะสม ทำให้ผลเฉลยโดยประมาณของรูปร่างการโก่งเดาะ และค่าแรงโก่งเดาะลู่เข้าสู่ผลเฉลยแม่นตรงอัตโนมัติโดยไม่ต้องทำการแบ่งชิ้นส่วนเพิ่มเติม   ในแต่ละรอบการทำซ้ำค่าลักษณะเฉพาะต่ำสุดสามารถคำนวณได้อย่างถูกต้องและมีประสิทธิภาพโดยเลือกใช้ระเบียบวิธีเชิงตัวเลขที่เหมาะสม จากนั้นนำระเบียบวิธีที่พัฒนาขึ้นไปวิเคราะห์หาค่าแรงโก่งเดาะของโครงสร้างประเภทต่างๆเพื่อยืนยันความถูกต้อง ศึกษาพฤติกรรมการลู่เข้า และแสดงขีดความสามารถในการวิเคราะห์ สุดท้ายนำเสนอและอภิปรายผลที่ได้จากการศึกษา
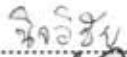
ภาควิชา วิศวกรรมโยธา   ลายมือชื่อนิสิต นิจวิชัย
สาขาวิชา วิศวกรรมโยธา   ลายมือชื่อ อ.ที่ปรึกษาวิทยานิพนธ์หลัก
ปีการศึกษา 2553

5270614421   : MAJOR CIVIL ENGINEERING

KEYWORDS :   FLEXURAL BUCKLING LOADS / COLUMNS /   EIGENVALUES /
ADAPTIVE BASIS FUNCTIONS / RAYLEIGH-RITZ APPROXIMATION

NIDVICHAI WATCHARKORN: DETERMINATION OF BUCKLING LOAD BY
ADAPTIVE SHAPE FUNCTIONS. ADVISOR: JAROON RUNGAMORNRAT,
Ph.D., 67 pp.

This study proposes the development of an accurate and powerful numerical technique capable of determining the flexural buckling load of two-dimensional skeleton structures. The key formulation is based upon the principle of stationary total potential energy whereas the discretization is adopted using standard Rayleigh-Ritz approximation. The crucial feature of the current technique is that a space of trial functions used in the approximation of the buckling shape is constructed from shape functions containing an adaptive parameter directly related to the member axial force and, more importantly, this space will contain the exact buckling shape if the member axial force is identical to its buckling load. Such special basis functions can be constructed, in an element-wise fashion, from a solution of the ordinary differential equation governing the buckling shape of a single element. In the present study, we propose a set of basis functions for several types of elements such as elements with and without lateral constraints, elements with consideration of shear deformation, and elements made of nonlinear materials. This integrated component enhances the capability of the buckling analysis of various types of structures (e.g. plane frames with and without lateral bracings, columns rested on an elastic foundation, inelastic buckling of columns, structures with significant shear deformation, etc.). With use of adaptive interpolation functions along with a proper iterative procedure, the approximate buckling shape and approximate buckling load automatically converge to the exact solutions without the need for mesh refinement. For any iteration, the minimum eigenvalue is efficiently and accurately computed by a selected numerical technique. The proposed method is then tested in the buckling analysis of many structures to demonstrate its accuracy, rate of convergence and capabilities. A selected set of numerical results are reported and discussed.

Department : Civil Engineering   Student's Signature ....

Field of Study : Civil Engineering   Advisor's Signature ....

Academic Year : 2010

ACKNOWLEDGEMENTS

CONTENTS

LIST OF TABLES

LIST OF FIGURES

Page

LIST OF ABBREVIATIONS

A area of cross section;

B, n material constants;

E modulus of elasticity;

E_T tangent modulus;

G shear modulus;

I moment of inertia;

k_1 first parameter of elastic foundation (Winkler foundation);

k_2 second parameter of elastic foundation;

$\mathbf{K}$ element stiffness matrices;

$\mathcal{K}$ unconstrained stiffness matrices of the structure;

$\hat{\mathcal{K}}$ reduced stiffness matrices;

L length of the member;

P axial load;

P_0 reference buckling load of the structure;

r roots of characteristic equation;

U strain energy functional;

v transverse displacement;

W load potential functional;

β rotation of the cross sectional;

γ shear angle of the cross section;

κ curvature;

λ shear correction factor;

Π total potential energy;

σ_0 reference stress;

ε_0 reference strain

CHAPTER I

INTRODUCTION

1.1 General

In design practice, buckling is commonly known as one of dominant modes of failure of structures consisting of slender, axially loaded members. Buckling is particularly dangerous because it can lead to catastrophic failure that generally provides no warning. A value of load associated with the buckling state is commonly defined as the load at which the structure switches from an equilibrium configuration in which all members remains straight to other equilibrium configurations where either certain or all members possess non-straight or twist configurations. In general, the load at buckling (as defined above) and the corresponding deformed configuration, known as the buckling mode shape, of structures containing perfectly straight, axially loaded members always exists but is not unique and depends primarily on various factors such as the geometry of the structure, loading patterns, boundary conditions, behavior of constituting materials, lateral constraints, etc. The lowest value among these loads is commonly termed the *buckling load* of the structure. Knowledge of the buckling load is not only useful in the design consideration of axially loaded slender structures but also essential in the analysis and design of structures subjected to combined axial and bending loads. For instance, in the recent design specification for steel buildings (e.g. ANSI/AISC 360-05), information of the elastic buckling load must be supplied to the design equations, in terms of the effective length factor, for both compression members and members in flexure and compression. Similarly, an interaction equation recommended by ACI 318-05 for designing long reinforced concrete columns under combined compression and bending moment also necessitates the effective length factor of those members. While the overall buckling behavior (e.g. the entire structure loosing their stability) depends primarily on the symmetry of the cross section and can be classified into several modes (e.g. ANSI/AISC 360-05; Salmon and Johnson, 1996; McCormac, 1994), e.g. flexural buckling, torsional buckling, flexural-torsional buckling, the flexural buckling has become one of the failure modes that is mostly encountered in

the design practice of compression members and beam-columns and is the main focus of the current investigation.

A method used to calculate the buckling load must be properly selected in order to provide reasonably accurate results with acceptable computational cost and effort. In general, techniques used in the analysis for the buckling load can be classified into three main categories, i.e. analytical techniques, semi-analytical technique, and numerical techniques. Analytical techniques, introduced since the toddler age of this area and continuously used until now, are based primarily on solving the governing differential equation along with determining a solution of the exact eigenvalue problem. Besides its positive feature to yield exact value of the buckling load, the method itself poses several drawbacks. For instance, the associated eigenvalue problem generally yields nonlinear equations involving functions of a transcendental form and, more importantly, it experiences mathematical difficulty when geometry of the structure, member properties and boundary conditions become increasingly complicated. In particular, as the complexity and number of characteristic equations increase, determination of the minimum eigenvalue in an analytical fashion is impossible.

To avoid the direct solving of governing differential equations and corresponding eigenvalue problems, an attractive alternative is to seek an explicit expression to estimate the buckling load. The most recognized, ready-for-use, analytical-based expression is Euler's formula, i.e. $P_{cr} = \pi^2 EI/(KL)^2$ where E represents Young's modulus, I is the area moment of inertia of the cross section, L denotes the unsupported length of the member, and K is a parameter reflecting the end conditions commonly termed the effective length factor (e.g. Timoshenko and Gere, 1961). Besides the popularity gaining from its simple form and the explicit indication of factors affecting the buckling load, this formula still possesses a major drawback associated with the difficulty to estimate the effective length factor K especially for columns in multi-story frames. A rough approximation of the effective length factor for columns in both sway and non-sway frames can be achieved by using alignment charts (e.g. Gaylord et al., 1992; McCormac, 1994). It should be noted however that due to several simplified

assumptions employed in the construction of such charts, the estimated effective length factor can be substantially deviated from the analytical solution. Work towards the improvement of the estimation of the effective length factor has been carried out continuously by various researchers who still fall in love with the beauty of Euler's formula (e.g. Aristizabal-Ochoa, 1994a; Aristizabal-Ochoa, 1994b; Hellesland et al., 1996a; Hellesland et al., 1996b; Gantes and Mageirou, 2005).

An improved version of the analytical technique, termed a semi-analytical technique, is to employ certain numerical procedures to aid the massive and complex computations associated with solving nonlinear equations while still maintain the analytical nature of the solution. The buckling load obtained from this technique is basically of comparable quality to the exact solution. However, similar to the analytical technique, its practical applications are still limited to structures of simple configurations.

Most powerful techniques applicable to the buckling analysis of various types of structures are based upon approximation theories (e.g. Galerkin approximation, Rayleigh-Ritz approximation, finite element approximation, etc.) along with appropriate numerical procedures. The formulation of the boundary value problem is normally established in a form well-suited for the approximation to be carried out in the general setting (e.g. weak formulation by either the weight residual technique or the principle of virtual work, variational formulation by the principle of stationary total potential energy, work and energy conservation equation, etc.). While techniques in this category possess less mathematical complexity in comparison with the analytical and semi-analytical methods and the rapid growth of their applications has been recognized nowadays, it still requires consideration of various computational aspects such as the approximation strategy, the solution method, and the implementation in terms of the computer software. The quality of approximate solutions depends primarily on the strategy and level of approximation and this requires special care to ensure the convergence and accuracy of the computed buckling loads.

It has no strong evidence to solidly identify the best among the three groups of techniques used for determining the buckling load of structures. It is generally problem dependent and, sometimes, the matter of preference. The key motivation of this proposed study is to seek a means to improve existing techniques for better estimation of the buckling load of a broad class of columns and frames. In the following section, results from extensive literature survey are presented in order to clearly define the objective and the scope of this study.

1.2 Literature Review

In this section, a brief overview of the background and existing work that are relevant to the current study is provided. The key objective is to demonstrate the sequence of historical development in this specific area and also provide sufficient evidence to identify available gap of knowledge. Results from literature survey are separated into three parts regarding to their main focus; the first part is associated with studies of elastic and inelastic flexural buckling loads of structures, the second part devoted to investigations of the influence of shear deformation on the flexural buckling behavior, and the last part summarizes work on buckling analysis of members with restraints against the lateral movement.

1.2.1 Elastic and inelastic flexural buckling analysis of structures

For several decades, mathematicians, researchers and engineers have proposed various approaches for determining flexural buckling load of column and frame structures. In 1744, Euler showed that there exists a critical load associated with the state where a perfectly straight, slender column under compression starts to admit another deformed equilibrium configuration; this critical load is later known as the buckling load. In his study, the column is only supported against the lateral movement at both ends and is compressed within the elastic range of a constituting material. For any value of axial load less than the buckling load, the column remains its straight and stable equilibrium configuration while, for any value of axial load larger than the buckling load, the straight equilibrium configuration becomes unstable and infinitesimally small

perturbation can push the column to a new stable equilibrium configuration. Since the Euler's era, the elastic buckling load (sometimes called the Euler's load to honor his first study in this area) of single columns with various end conditions and more complex structures have been extensively investigated (see Timoshenko and Gere, 1961).

One important drawback of the Euler's formula is its limited practical applications resulting from the linear elasticity assumption. More precisely, the constituting material is assumed to remain in a linear regime both prior to and at the onset of buckling. Elastic buckling can occur only for very slender columns while most columns found in practices buckle within an inelastic range. To enable the Euler's formula to treat inelastic buckling, the concept of variable modulus of elasticity has been introduced (e.g. Engesser, 1889; Engesser, 1891; Considère, 1891). In 1889, Engesser proposed a well-known tangent modulus theory. In his investigation, the column was assumed to remain straight until the onset of buckling, and the tangent modulus was assumed to be constant throughout the cross section. Based on the tangent modulus theory, the Euler's buckling formula can be modified by simply replacing the Young modulus by the tangent modulus at a stress level at the onset of buckling. Later, Engesser (1995) pointed out that his original tangent modulus theory is invalid, and he then replaced it by the reduced modulus or the double modulus theory. Based on the latter theory, fibers on the convex side of a bent column undergo elastic unloading (or strain reversal) while those on the concave side experience inelastic loading. With this new assumption, the theory was anticipated to better predict the inelastic buckling load; however, experimental evidences tended to flavor the tangent modulus theory while the reduced modulus theory generally yields higher buckling loads than test results. Later, in 1946, Shanley drew significant attention to the erroneous assumption of the reduced modulus theory; i.e. a column is always assumed to remain perfectly straight up to the reduced modulus load. To support his argument, Shanley proposed a model of two columns connecting at its two rigid ends by a spring at the center. He pointed out that an initially straight column will buckle at the tangent modulus load and will continue to bend with increasing axial load. With the Shanley concept, the tangent modulus theory

provides a lower bound of the column strength, i.e. the load at which an initially straight column will start to bend. On the contrary, the reduced modulus theory leads to the upper bound of the buckling load since the reduced modulus load can be achieved only when the column is temporarily supported until reaching that load.

To estimate the elastic and inelastic flexural buckling loads of both single columns and frames, various techniques have been proposed since the first study by Euler in 1744. A classical approach that has been utilized extensively and continuously since its early age is based upon an analytical technique. The key step is to solve the governing differential equation for a correct function form describing the buckling shape and then employ the boundary conditions to form an eigenvalue problem. This technique has proven successful for determining the buckling load of single columns with various end conditions and frames with simple configurations (e.g. Timoshenko and Gere, 1961; Chajes, 1974; Chen and Lui, 1987). To treat more complex structures, Mahfouz (1999) proposed a semi-analytical technique using stability functions of each member to form a set of exact characteristic equations of the entire structure and the minimum eigenvalue (elastic buckling load) was searched by increasing an axial loading parameter from zero until reaching the point where the determinant of the characteristic matrix changes sign. While Mahfouz's approach can yield results of comparable accuracy to the exact solution, the computational cost related to calculations of the matrix determinant and a large number of iteration can be significant.

To enhance the capability of the analytical and semi-analytical techniques to treat a broader class of structures, various approximate techniques have been proposed. Two of these techniques include the use of Rayleigh-Ritz strategy to approximate the buckling shape in the conservation of work and energy equation (e.g. Chajes, 1974) and in the principle of stationary total potential energy (e.g. Dawe, 1984; Hughes, 1987). In such techniques, the buckling shape of the structure was assumed a priori to establish a set of characteristic equations governing the approximate buckling load. While they are of less mathematical complexity in comparison with the analytical method, they generally yield the buckling load higher than the exact value. Another key

disadvantage of the Rayleigh-Ritz approximation is that there is no systematic means to choose the space of trial functions to ensure the accuracy and convergence of the approximate solution. Another powerful numerical procedure for buckling load analysis is the finite element method (FEM) (e.g. Dawe, 1984; Yang, 1986; Hughes, 1987); this particular technique can be viewed as the improved version of the Rayleigh-Ritz approximation. A space of trial buckling shapes is systematically constructed based on simple functions defined in an element-wise fashion. Nevertheless, convergence and accuracy of the approximate buckling load must still be confirmed by numerical experiments on a series of meshes. It is also important to emphasize that use of simple functions to represent the buckling shape can pose a potential drawback to this technique; for instance, a large number of elements may be required to accurately capture the complex buckling shape and this can result in a substantial computational cost. Other numerical and approximate techniques used to investigate flexural buckling problems have also been adopted; some of them are summarized below.

Gantes and Mageirou (2005) proposed a scheme to improve the estimation of an effective length factor of columns in multi-story sway frames. In their technique, a frame is modeled as an individual column with a rotational spring at both ends. A slope-deflection method was utilized to derive the expression of the spring rotational stiffness for all possible boundary conditions at the far end, with and without the axial force. The simplified version of the derived rotational stiffness is also obtained via the use of Taylor series expansion. In 2007, Girgin and Ozmen presented a simplified procedure for determining the buckling loads of three-dimensional frames. In their work, the principle of virtual work and Betti's reciprocal theorem were employed and it finally led to a single equation governing the buckling load:

$$W_1 = W_2 \tag{1.1}$$

where W_1 is the virtual work of forces from a system I (under axial loading) due to the displacement from a system II (under lateral loading) and W_2 is the virtual work of forces from the system II due to the displacement from the system I. It is worth noting

that while the displacement from both systems were taken to be identical in such calculations, the displacement from the system I represents the relative column displacement whereas that from the system II corresponds to the story displacement. This proposed technique has been found applicable to both regular and irregular structures; however, it still requires to compute the displacements of the system II and values of the approximate buckling load depends primarily on the choice of lateral loads applied to that system.

Later, Yoo and Choi (2008) proposed a new method for analysis of inelastic buckling of steel frames. Their method utilized standard eigenvalue analysis along with the tangent modulus theory and a column strength curve. The first iteration of this method requires performing linear stress analysis to determine the internal force and bending moments of all members. The eigenvalue at the first step was set equal to the eigenvalue obtained from elastic buckling analysis and the minimum eigenvalue was then employed to obtain the flexural and axial resistances from a column strength curve. Next, the tangent modulus of each member was obtained from the axial and flexural information and then used to construct the stiffness matrix for the next search of the minimum eigenvalue. When the convergence was achieved, the computed eigenvalue was utilized to find the critical load of the steel frame. Note in addition that the geometric imperfection present in each member can be treated via the use of a column strength curve.

Recently, Choi and Yoo (2009) developed a technique to improve the accuracy of the effective length factor for multi-story frames. The traditional iterative buckling approach can predict reasonably accurate effective length factors only for columns in the weakest story or the weakest member of the frame. The weakest story or the weakest member was defined as a story or a member that is critical and controls the overall buckling of the frame or, equivalently, a story or a member possessing the maximum stiffness parameter, $L\sqrt{P/EI}$. To enhance performance of the traditional approach, they introduced a fictitious axial force by considering both the most influential member (with the maximum stiffness parameter) and the least influential member (with

the minimum stiffness parameter). A formula proposed for estimating such fictitious axial force was given by

$$\delta P = \frac{E_{li}I_{li}}{E_{mi}I_{mi}} \left(\frac{K_{mi}L_{mi}}{\bar{K}_{li}L_{li}} \right)^2 P_{mi} - P_{li}$$ (1.2)

The first step of this approach involves solving a conventional eigenvalue problem to obtain an increment of the fictitious axial force by comparing the stiffness parameter given by (1.2). Next, the axial force for all members is modified and the new geometric stiffness matrix is recalculated for the next search of the minimum eigenvalue. Once the new minimum eigenvalue is obtained, the effective length factor for all members is computed following by their convergence check. For the next iteration, the increment of the fictitious force is not required for members whose effective length factor is already converged. The process is to be continued until the convergence of the effective length factor is achieved for all members.

1.2.2 Buckling analysis of structures with consideration of shear deformation

Shear deformation has been considered as one of important factors that play an important role in the behavior of flexural buckling of columns and frames. Engesser (1891) was recognized the first who investigated the influence of shear deformation on the buckling load of a straight bar and suggested the modification to the original Euler's differential equation that governs the buckling shape. All internal force measures in Engesser's approach were based on the undeformed state as shown in Figure 1.1(a); more specifically, the axial force N_1 acts in the direction of the member axis and the shear force Q_1 acts in the tangential direction of the cross section. The other different and well-recognized model was proposed by Haringx in 1948. In Haringx's approach, all internal forces were measured based on the deformed state as depicted in Figure 1.1(b). Unlike the former approach, the axial force N_2 was assumed to be normal to the rotating cross section and the shear force Q_2 was assumed to be in the tangential direction of the rotating cross section.

(a)   (b)
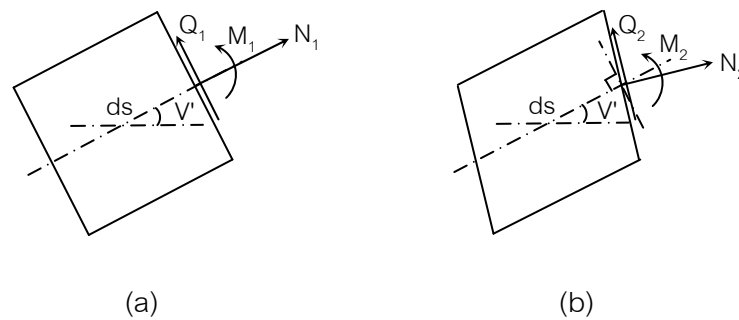
Figure 1.1 Two different measures for all internal forces within cross section: (a)

Engesser's approach and (b) Haringx's approach

These two models have been extensively employed by various investigators to study the influence of shear deformation on the buckling behavior (e.g. Timoshenko and Gere, 1961; Ziegler, 1982; Djukic and Atanackovic, 1993; Wang et al., 2002; Blaauwendraad, 2008). Timoshenko and Gere (1961) utilized both Engesser and Haringx's approaches in the buckling analysis of columns. They pointed out that the Haringx's approach can lead to more accurate results when the effect of shear deformation is significantly large (e.g. the buckling of helical springs) while the Engesser's approach yields results on the safe side. Ziegler (1982) further examined those two approaches by comparing with a more fundamental method based on analytical mechanics. He concluded in his study that the Engesser's approach is superior to the Haringx's approach for analysis of buckling of bars. In particular, he also explained why the Haringx's method predicts accurate results for the buckling of springs. Later, Djukic and Atanackovic (1993) investigated the buckling behavior of a hinged-hinged column by taking shear deformation into account. In their approach, the axial force was assumed to direct along the rod axis (the same as the Engesser's approach) while the shear force assumed the direction normal to the deformed axis. It was found from this study that results were in close agreement with those obtained from the Engesser's approach.

Wang et al. (2002) employed an analytical technique (i.e. solving the differential equation for the buckling shape and exact eigenvalue problem for the buckling load) to establish the exact stability criteria and obtain the buckling load of

Timoshenko columns subjected to interior and end axial loads for various types of boundary conditions. The influence of shear deformation, boundary conditions, and magnitudes and positions of the interior load on values of the buckling load was fully investigated. Results revealed that the effect of transverse shear deformation becomes significant when a column is subjected to the interior load near its base. In this particular situation, the column behaves in the same way as a stocky column. It was also found that the effect of transverse shear deformation in lowering the buckling load is more apparent for columns with greater restraints at their ends. In 2008, Blaauwendraad showed that the Haringx's approach yields a wrong limit of the buckling load for very weak-in-shear beam-columns. He supported his argument by considering a simply-supported Timoshenko beam-column with a semi-rigid connection and a spring support at its mid-span. His results indicated that the buckling load obtained from the Engesser's and Haringx's approaches are comparable in magnitude when the shear rigidity of a column is large. However, when a column has the weak shear rigidity, the buckling load obtained from the Haringx's approach significantly deviates from that for the limiting case of a column with infinitely large flexural rigidity and finite shear rigidity.

1.2.3 Buckling analysis of members with restraints against lateral movement

Beams and columns supported laterally along their length are very common in structural configuration, e.g. beams resting on an elastic foundation and columns braced against the lateral movement. A well-known mathematical model used to describe an elastic support is proposed by Winkler (1867) and later named to honor him as *Winkler* foundation. In this model, the foundation acts as if it consists of an infinite number of closely spaced linear springs, and its constitutive behavior is completely characterized by a single parameter termed the foundation modulus k. To enhance the Winkler model, some investigators included, in addition, the interactions between the elastic spring and the foundation and this, therefore, leads to one additional parameter. Several equivalent two-parameter elastic foundation models have been found in the literature, e.g. Filonenko-Borodich foundation, Pasternak foundation, generalized foundation and Vlasov foundation. The Filonenko-Borodich foundation was first

proposed by Filonenko-Borodich (1940). In this model, the top end of springs is attached to an elastic membrane that is pre-stretched by a constant tension T. The Pasternak foundation, proposed by Pasternak (1954), takes the shear interactions among the springs into account. Specifically, the top end of the springs is attached to an incompressible layer that can resist only the transverse shear deformation. In 1964, Kerr proposed the generalized foundation model by assuming that at each contact point, there are both the pressure and moment acting to the foundation. The Vlasov foundation, developed by Vlasor and Leontiev (1966), was mathematically complicated for its original version. A simplified model was later introduced and has been widely used. For all two-parameter models described above, their behavior is governed by the same equation as follows:

$$p(x) = k_1 w(x) - k_2 \frac{d^2 w(x)}{dx^2} \tag{1.3}$$

where $p(x)$ denotes the reaction normal to the foundation, $w(x)$ represents the lateral or transverse deflection, and k_1 and k_2 are model parameters. Note that for the Winkler foundation, the parameter k_2 is taken to be zero.

On the basis of extensive literature survey, above models have been used extensively in the analysis of beams and columns resting on the elastic foundation. Zhaohua and Cook (1983) employed the finite element method to analyze beams on both single-parameter and two-parameter foundations. Two types of elements, one is based on the exact displacement function and the other is based on a cubic displacement function, were developed in their study. It was found that use of elements based on the exact displacement function in the discretization yields exact solution for all deformation and internal forces without mesh refinement but use of elements based on the cubic displacement function gives only approximate solutions with their accuracy depending upon the level of refinement. Later, Yankelevsky and Eisenberger (1986) applied a direct analytical technique to derive an exact stiffness matrix for a beam-column resting on an elastic Winkler foundation. Eisenberger et al. (1986) also derived the elastic and geometric stiffness matrices for a beam-column resting on an elastic

Winkler foundation. By using these matrices, they were able to determine the buckling loads and the corresponding buckling mode shapes of a continuous column on an elastic foundation.

In 1988, Cheng and Pantelides presented the buckling load and buckling mode shape of a simple Timoshenko beam-columns supported laterally by an elastic foundation. In their study, two approaches were employed to derive the governing differential equations, stiffness coefficients, and fixed-end forces. The first approach was based upon the Haringx's model with the shear component being calculated from the total slope, while the second approach was based upon the Engesser's model with the shear component being computed differently from the bending slope. They observed from this study that values of the buckling load for columns with relatively small slenderness ratio are significantly reduced when the shear deformation is included, and the first approach always yields the buckling load less than the second approach. In particular, when the slenderness ratio is reduced, the buckling load predicted by the Haringx's and Engesser's models exhibits significant discrepancy.

In 1995, Naidu and Rao used the finite element method to study the stability behavior of prismatic columns resting on a two-parameter elastic foundation. The constant of a shearing layer for the two halves of a column was taken to have different values and various boundary conditions were considered. In 2000, Seemapholkul developed a technique based on the finite element method to determine the buckling load of a Timoshenko beam-column resting on a two-parameter Filonenko-Borodich foundation with consideration of shear deformation via the Engesser's model. In the finite element approximation, the exact element shape functions obtained by solving a Timoshenko beam analytically (in the absence of an axial load) were utilized. Their technique was found promising and yielded accurate results upon proper mesh refinement. Recently, Xia and Zhang (2009) derived a governing differential equation for a simply-supported beam-column resting on the Winkler foundation. By directly solving the differential equation and the corresponding eigenvalue problem, they could obtain

the buckling load of such beam-column and then confirmed their results with those by a reliable finite element program.

Based on extensive review of relevant work in this area and the great contribution of knowledge to practical applications, it has no doubt that the development of accurate and powerful numerical techniques to compute the buckling load of both columns and frames by taking various factors such as the inelastic effect, shear deformation, and restraints against the lateral movement into account is essential and still requires further investigations. One potential improvement to existing methods, and is the main focus of this study, is to supply the automatic adaptivity of the approximation that allows the exact buckling load be achieved without any mesh refinement.

1.3 Research Objective

The key objective of this investigation is to develop an efficient and accurate numerical technique to estimate the buckling load of two-dimensional skeleton structures.

1.4 Scope of Research

The present research has been carried out within following context and assumptions:

1) Structures are two-dimensional and consist of straight and prismatic one-dimensional members.

2) Initial imperfections such as initial crookedness, eccentric loads, and residual stress are not included.

3) Only flexural buckling is considered.

4) The constituting material can be either linear elastic or inelastic. For elastic materials, the Young's modulus is prescribed and for inelastic materials, the tangent modulus is known.

5) Effect of shear deformation is included by using Engesser' model.

6) Influence of point restraints against the lateral movement and rotation is considered using translational and rotational spring models.

7) Influence of uniformly distributed lateral restraints is considered using a two-parameter foundation model.

8) Influence of axial deformation is neglected.

1.5 Research Methodology

The key task of this research is associated with the development of a numerical procedure to have capabilities for analysis of the buckling load of structures. Methodology employed to accomplish such task can be described as follows:

1) The principle of stationary total potential energy is employed to establish the variational formulation governing the buckling problem,

2) The Rayleigh-Ritz approximation is adopted to derive the approximate characteristic equations for an individual element,

3) Space of trial functions used in the approximation of the buckling shape is based on adaptive basis functions derived from the exact solution of the ordinary differential equation governing the buckling shape,

4) Standard assembly procedure is employed to form an approximate eigenvalue problem for the entire structure,

5) A power method supplemented by Rayleigh quotient is utilized to calculate the minimum eigenvalue, and

6) A selected iterative procedure is employed, along with adaptive buckling shape, to achieve the accurate buckling load.

1.6 Research Significance

An important output gained from this study is an accurate and efficient numerical procedure capable of determining the flexural buckling loads and other relevant buckling information such as the effective length factor of various structures typically encountered in practices, e.g. multi-story non-sway and sway frames, columns resting on elastic foundations, buckling of piles, etc. The most attractive feature of the proposed technique is the use of a special space of trial functions that allows the automatic adaptivity to enhance the accuracy of approximate solutions. Results

obtained from this technique are of high quality and, generally, comparable to the analytical solutions. As a consequence, results generated from the current technique can be used as benchmark solutions for verification and comparison purposes. Another direct application is to employ this technique to enhance the estimation of the effective length factor, instead of using an old-style approach via the alignment charts, in the design of compression members and members in combined flexure and compression.

CHAPTER II

THEORETICAL CONSIDERATIONS

In this chapter, several theoretical aspects relevant to the present study including the problem statement, the variational formulation for a buckling problem by the principle of stationary total potential energy, construction of an approximate characteristic equation by a Rayleigh-Ritz approximation scheme, a direct assembly procedure to form a discretized eigenvalue problem for the entire structure, and the construction of adaptive shape functions used in the approximation of the buckling shape, are summarized.

2.1 Problem statement

Consider a two-dimensional, axially loaded, initial-imperfection free, skeleton structure as shown schematically in Figure 2.1. The structure can consist of either a single prismatic member or multiple prismatic members with different cross sectional properties. In addition, for each individual member, restraints against the lateral movement or rotation, modeled either by a concentrated elastic spring or the uniformly distributed elastic spring, may be present. All members are assumed to be made of homogeneous and isotropic materials. The overall structure is properly constrained to prevent all possible in-plane rigid body motions whereas it is fully constrained against the out-of-plane displacement.
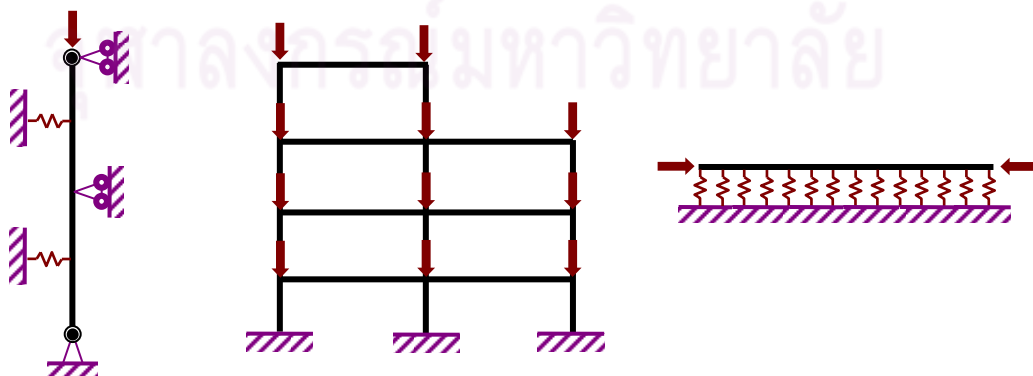
Figure 2.1 Two dimensional axially loaded structures focused in the current investigation

The problem statement, for this particular study, is to determine the flexural buckling load of structures described above by including the influence of the lateral restraint, shear deformation and nonlinear behavior of constituting materials in the mathematical model. The influence of axial deformation is assumed to be relatively small and is therefore discarded in the current investigation.

2.2 Variational formulation

A variational formulation governing the flexural buckling load of a structure defined in the problem statement is established using the principle of stationary total potential energy as briefly described below.

At the onset of buckling, the load potential functional associated with the axial load in the member undergoing the axial shortening resulting only from the curvature, denoted by $\mathbf{W}$, is given by

$$\mathbf{W} = -\sum_{i=1}^{m} \frac{1}{2} \int_{0}^{L_i} P_i \left(\frac{dv}{dx} \right)^2 dx \tag{2.1}$$

where $v = v(x)$ is the transverse displacement (or deflection) of a member, $\mathbf{m}$ is the number of axially loaded members in the structure, and L_i and P_i are the length and axial load of the ith member, respectively. The strain energy functional of the structure, denoted by $\mathbf{U}$, due to bending deformation, shear deformation and deformation of elastic lateral restraints is given by (see also the work of Seemapholkul, 2000)

$$U = U_b + U_s + U_l \tag{2.2}$$

where

$$U_b = \sum_{i=1}^{m} \frac{1}{2} \int_{0}^{L_i} E_i I_i \kappa_i^2 dx \tag{2.3a}$$

$$U_s = \sum_{i=1}^{m} \frac{1}{2} \int_{0}^{L_i} \lambda_i G_i A_i \gamma_i^2 dx \tag{2.3b}$$

$$U_1 = \sum_{i=1}^{m} \frac{1}{2} \int_0^{L_i} k_{1i} v^2 dx + \sum_{i=1}^{m} \frac{1}{2} \int_0^{L_i} k_{2i} \left(\frac{dv}{dx}\right)^2 dx \qquad (2.3c)$$

where U_b is the strain energy due to bending deformation, κ_i is the curvature, and $E_i I_i$ is the flexural rigidity of the cross section at the onset of buckling; U_s is the strain energy due to shear deformation, γ_i is the shear angle of the cross section, and λ_i and $G_i A_i$ are the shear correction factor and the shear rigidity of the cross section; and U_l is the strain energy due to deformation of elastic lateral restraints and k_{1l} and k_{2l} are constants associated with the two-parameter foundation model (1.3). From kinematics, the curvature and shear angle at any cross section can be related to the transverse displacement v and the rotation of the cross sectional β by

$$\gamma_i = \frac{dv}{dx} - \beta \qquad (2.4)$$

$$\kappa_i = \frac{d\beta}{dx} \qquad (2.5)$$

where dv/dx represents the slope of the member axis. The total potential energy of the structure at the onset of the buckling, denoted by Π, is given by

$$\Pi = U + W \qquad (2.6)$$

From the principle of stationary total potential energy, the deformed state is an equilibrium state if and only if the total potential energy is stationary or, equivalently, the first variation of Π must identically vanish, i.e.

$$\delta\Pi = \delta U + \delta W = 0 \qquad (2.7)$$

where δ denotes the first variation of a functional. It is worth noting that equation (2.7) is in fact the static equilibrium equation of the structure formulating based on the deformed configuration. By inserting equations (2.1) and (2.2) into equation (2.7), it leads to

$$\sum_{i=1}^{m} \int_0^{L_i} E_i I_i \kappa_i \delta\kappa_i dx + \sum_{i=1}^{m} \int_0^{L_i} \lambda_i G_i A_i \gamma_i \delta\gamma_i dx + \sum_{i=1}^{m} \int_0^{L_i} k_{1i} v\delta v dx + \sum_{i=1}^{m} \int_0^{L_i} k_{2i} v'\delta v' dx = \sum_{i=1}^{m} \int_0^{L_i} P_i v'\delta v' dx$$

$$(2.8)$$

The weak-form equation (2.8) forms a basis for the development of an approximate characteristic equation to estimate the flexural buckling load.

2.3 Characteristic equation for single element
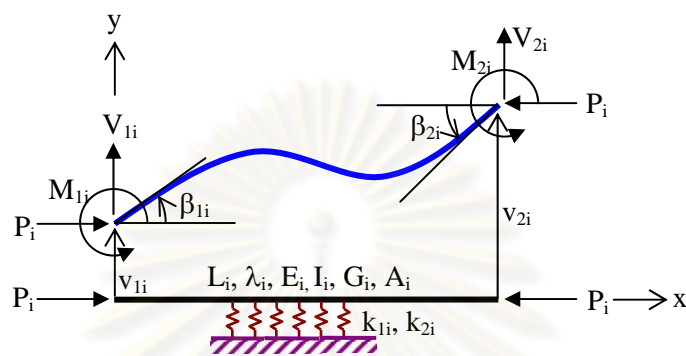
Figure 2.2 Undeformed and deformed configurations of generic i^{th} element of length L_i, axial load P_i, and properties $\{E_i, I_i, \lambda_i, G_i, A_i, k_{1i}, k_{2i}\}$

Consider the generic i^{th} element of length L_i, axial load P_i, and properties $\{E_i, I_i, \lambda_i, G_i, A_i, k_{1i}, k_{2i}\}$. Its undeformed configuration and deformed configuration at the onset of buckling are illustrated in Figure 2.2. The total potential energy of this generic member due to all effects at the buckling state is given by

$$\Pi_i = \frac{1}{2}\left\{\int_0^{L_i} E_i I_i \kappa_i^2 dx + \int_0^{L_i} \lambda_i G_i A_i \gamma_i^2 dx + \int_0^{L_i} k_{1i} v^2 dx + \int_0^{L_i} k_{2i} v'^2 dx - \int_0^{L_i} P_i v'^2 dx\right\}$$
$$- V_{1i} v_{1i} - M_{1i}\beta_{1i} - V_2 v_{2i} - M_2\beta_{2i} \tag{2.9}$$

where $\{V_{1i}, M_{1i}, V_{2i}, M_{2i}\}$ denote the shear forces and bending moments at both ends of the member induced in the deformed state and $\{v_{1i}, \beta_{1i}, v_{2i}, \beta_{2i}\}$ denote the transverse displacements and cross sectional rotations at both ends of the member. Note that the last four terms on the right hand side of (2.9) are associated with the load potential produced by $\{V_{1i}, M_{1i}, V_{2i}, M_{2i}\}$. For the deformed state $v = v(x)$ and $\beta = \beta(x)$ to be an equilibrium state, the total potential energy Π_i must be stationary, i.e.

$$\delta\Pi_i = \int_0^{L_i} E_i I_i \kappa_i \delta\kappa_i dx + \int_0^{L_i} \lambda_i G_i A_i \gamma_i \delta\gamma_i dx + \int_0^{L_i} k_{1i} v\delta v dx + \int_0^{L_i} k_{2i} v'\delta v' dx - \int_0^{L_i} P_i v'\delta v' dx$$

$$-V_{1i}\delta v_{1i} - M_{1i}\delta\beta_{1i} - V_2\delta v_{2i} - M_2\delta\beta_{2i} = 0 \tag{2.10}$$

By following Rayleigh-Ritz approximation, the buckling shape of the member is approximated by

$$v(x) = \psi_1(x)v_{1i} + \psi_2(x)\beta_{1i} + \psi_3(x)v_{2i} + \psi_4(x)\beta_{2i} \tag{2.11}$$

$$\beta(x) = \widehat{\psi}_1(x)v_{1i} + \widehat{\psi}_2(x)\beta_{1i} + \widehat{\psi}_3(x)v_{2i} + \widehat{\psi}_4(x)\beta_{2i} \tag{2.12}$$

where $\psi_i(x)$ and $\widehat{\psi}_i(x)$ are prescribed shape functions. By substituting (2.11) and (2.12) into (2.10) and then employing arbitrariness of $\{\delta v_{1i}, \delta\beta_{1i}, \delta v_{2i}, \delta\beta_{2i}\}$, it leads to a set of characteristic equations for the ith member:

$$\left(\mathbf{K}_{bi} + \mathbf{K}_{si} + \mathbf{K}_{l1i} + \mathbf{K}_{l2i} - \mathbf{K}_{gi}\right)\mathbf{u} = \mathbf{f} \tag{2.13}$$

where $\mathbf{u} = \{v_{1i}, \beta_{1i}, v_{2i}, \beta_{2i}\}^{\top}$ is a vector containing nodal degrees of freedom of the member, $\mathbf{f} = \{V_{1i}, M_{1i}, V_{2i}, M_{2i}\}^{\top}$ is a vector of member end forces, $\mathbf{K}_{bi}$, $\mathbf{K}_{si}$, $\mathbf{K}_{l1i}$, $\mathbf{K}_{l2i}$, and $\mathbf{K}_{gi}$ are element stiffness matrices with their entries defined by

$$\left[\mathbf{K}_{bi}\right]_{mn} = \int_0^{L_i} E_i I_i \widehat{\psi}'_m \widehat{\psi}'_n dx \tag{2.14}$$

$$\left[\mathbf{K}_{si}\right]_{mn} = \int_0^{L_i} \lambda_i G_i A_i \left(\psi'_m - \widehat{\psi}_m\right)\left(\psi'_n - \widehat{\psi}_n\right) dx \tag{2.15}$$

$$\left[\mathbf{K}_{l1i}\right]_{mn} = \int_0^{L_i} k_{1i} \psi_m \psi_n dx \tag{2.16}$$

$$\left[\mathbf{K}_{l2i}\right]_{mn} = \int_0^{L_i} k_{2i} \psi'_m \psi'_n dx \tag{2.17}$$

$$\left[\mathbf{K}_{gi}\right]_{mn} = \int_0^{L_i} P_i \psi'_m \psi'_n dx \tag{2.18}$$

where $[\mathbf{A}]_{mn}$ denotes an entry located at the mth row and the nth column of a matrix $\mathbf{A}$. By introducing a relation $P_i = \alpha_i P_0$ where P_0 is a reference axial load and α_i is a load scaling factor for the ith member, the characteristic equations (2.13) now become

$$\left(\mathbf{K}_{bi} + \mathbf{K}_{si} + \mathbf{K}_{l1i} + \mathbf{K}_{l2i} - P_0\hat{\mathbf{K}}_{gi}\right)\mathbf{u} = \mathbf{f} \tag{2.19}$$

where $\hat{\mathbf{K}}_{gi}$ is defined by

$$\left[\hat{\mathbf{K}}_{gi}\right]_{mn} = \int_0^{L_i} \alpha_i \psi'_m \psi'_n dx \tag{2.20}$$

2.4 Discretized eigenvalue problem for entire structure

By employing equilibrium and continuity at all nodes of the structure, the characteristic equations (2.19) for all members can be assembled into a set of characteristic equations for the entire structure using the same procedure as that for the direct stiffness method (e.g. Gallagher et al., 2000; Kassimali, 2005). The global characteristic equation can be expressed in a matrix form by

$$\left(\mathcal{K}_b + \mathcal{K}_s + \mathcal{K}_{l1} + \mathcal{K}_{l2} - P_0\mathcal{K}_g\right)\mathbf{U} = \mathbf{F} \tag{2.21}$$

where $\mathcal{K}_b$, $\mathcal{K}_s$, $\mathcal{K}_{l1}$, $\mathcal{K}_{l2}$ and $\mathcal{K}_g$ are unconstrained stiffness matrices of the structure resulting from the direct assembly of $\mathbf{K}_{bi}$, $\mathbf{K}_{si}$, $\mathbf{K}_{l1i}$, $\mathbf{K}_{l2i}$, and $\hat{\mathbf{K}}_{gi}$, respectively, $\mathbf{U}$ is a vector of nodal degrees of freedom of the corresponding unconstrained structure, and $\mathbf{F}$ is a vector of nodal forces. It is worth noting that for buckling problems, all entries of the vector $\mathbf{F}$ vanishes except those associated with the constrained degrees of freedom where non-zero reactions induced during buckling may exist. By further enforcing the essential boundary conditions at all supports via proper removal of rows and columns of $\mathcal{K}_b$, $\mathcal{K}_s$, $\mathcal{K}_{l1}$, $\mathcal{K}_{l2}$ and $\mathcal{K}_g$, it leads to a discretized eigenvalue problem governing the approximate reference buckling load of the structure P_0:

$$\left(\hat{\mathcal{K}}_b + \hat{\mathcal{K}}_s + \hat{\mathcal{K}}_{l1} + \hat{\mathcal{K}}_{l2} - P_0\hat{\mathcal{K}}_g\right)\hat{\mathbf{U}} = \mathbf{0} \tag{2.22}$$

where $\hat{\mathcal{K}}_b$, $\hat{\mathcal{K}}_s$, $\hat{\mathcal{K}}_{l1}$, $\hat{\mathcal{K}}_{l2}$, $\hat{\mathcal{K}}_g$ and $\hat{\mathbf{U}}$ are reduced stiffness matrices and a vector of free degrees of freedom after the treatment of essential boundary conditions.

2.5 Construction of special basis functions

Another crucial component of the present study is a set of adaptive shape functions used in the Rayleigh-Ritz approximation (2.11)-(2.12). These shape functions can be constructed directly from an exact solution of the ordinary differential equations governing the buckling shape of each member as described below.

First, the differential equations governing the buckling shape $v = v(x)$ and $\beta = \beta(x)$ of the ith member can readily be obtained by applying the stationary principle (2.10) along with the relations (2.4)-(2.5) and the arbitrariness of $\delta v(x)$ and $\delta\beta(x)$ (see details of derivation in Seemapholkul, 2000). This finally leads to a pair of fully coupled differential equations

$$(P_i - k_{2i} - \lambda_i G_i A_i)\frac{d^2 v}{dx^2} + \lambda_i G_i A_i \frac{d\beta}{dx} + k_{1i} v = 0 \tag{2.23}$$

$$E_i I_i \frac{d^2\beta}{dx^2} + \lambda_i G_i A_i \left(\frac{dv}{dx} - \beta\right) = 0 \tag{2.24}$$

By taking derivative of (2.23) with respect to x and then solving for $d^2\beta / dx^2$, it yields

$$\frac{d^2\beta}{d\overline{x}^2} = \left(1 - \overline{\eta}_i \overline{P}_i + \overline{\eta}_i \overline{k}_{2i}\right)\frac{d^3\overline{v}}{d\overline{x}^3} - \overline{\eta}_i \overline{k}_{1i} \frac{d\overline{v}}{d\overline{x}} \tag{2.25}$$

where $\overline{x} = x / L$, $\overline{v} = v / L$, $\overline{\eta}_i = E_i I_i / \lambda_i G_i A_i L_i^2$, $\overline{P}_i = P_i L_i^2 / E_i I_i$, $\overline{k}_{1i} = k_{1i} L_i^4 / E_i I_i$ and $\overline{k}_{2i} = k_{2i} L_i^2 / E_i I_i$. By inserting (2.25) into (2.24), we then obtain the explicit expression for the rotation β in terms of the displacement v as

$$\beta = \overline{\eta}_i \left(1 - \overline{\eta}_i \overline{P} + \overline{\eta}_i \overline{k}_{2i}\right)\frac{d^3\overline{v}}{d\overline{x}^3} + \left(1 - \overline{\eta}_i^2 \overline{k}_{1i}\right)\frac{d\overline{v}}{d\overline{x}} \tag{2.26}$$

By substituting (2.26) into (2.23), it leads to a governing differential equation for the displacement $\overline{v}$:

$$\frac{d^4\overline{v}}{d\overline{x}^4} + 2\overline{\varpi}\frac{d^2\overline{v}}{d\overline{x}^2} + \overline{\xi}\overline{v} = 0 \tag{2.27}$$

where

$$\overline{\varpi} = \frac{\left(\overline{P}_i - \overline{k}_{2i} - \overline{\eta}_i \overline{k}_{1i}\right)}{2\left(1 - \overline{\eta}_i \overline{P}_i + \overline{\eta}_i \overline{k}_{2i}\right)} \tag{2.28}$$

$$\overline{\xi} = \frac{\overline{k}_{1i}}{\left(1 - \overline{\eta}_i \overline{P}_i + \overline{\eta}_i \overline{k}_{2i}\right)} \tag{2.29}$$

The general solution of equation (2.27) takes the form

$$\overline{v}(\overline{x}) = C_1 e^{r_1 \overline{x}} + C_2 e^{r_2 \overline{x}} + C_3 e^{r_3 \overline{x}} + C_4 e^{r_4 \overline{x}} \tag{2.30}$$

where C_1, C_2, C_3 and C_4 are arbitrary constant and r_1, r_2, r_3 and r_4 are distinct roots of the following characteristic equation:

$$r^4 + 2\overline{\varpi} r^2 + \overline{\xi} = 0 \tag{2.31}$$

By substituting (2.30) into (2.26), we then obtain

$$\beta(\overline{x}) = \overline{C}_1 e^{r_1 \overline{x}} + \overline{C}_2 e^{r_2 \overline{x}} + \overline{C}_3 e^{r_3 \overline{x}} + \overline{C}_4 e^{r_4 \overline{x}} \tag{2.32}$$

where

$$\overline{C}_m = \left\{ \overline{\eta}_i \left(1 - \overline{\eta}_i \overline{P}_i + \overline{\eta}_i \overline{k}_{2i}\right) r_m^3 + \left(1 - \overline{\eta}_i^2 \overline{k}_{2i}\right) r_m \right\} C_m \tag{2.33}$$

By enforcing following essential boundary conditions at the both ends of a member

$$\overline{v}(0) = v_{1i}/L \tag{2.34a}$$

$$\beta(0) = \beta_{1i}/L \tag{2.34b}$$

$$\overline{v}(1) = v_{2i}/L \tag{2.34c}$$

$$\beta(1) = \beta_{2i}/L \tag{2.34d}$$

along with using the relation (2.34), it yields a system of linear algebraic equations for C_i. Once C_i are solved and $\overline{C}_i$ are determined from (2.33), they are inserted into (2.30) and (2.32) to obtain the buckling shape in terms of the nodal degrees of freedom $\{v_{1i}, \beta_{1i}, v_{2i}, \beta_{2i}\}$:

$$\overline{v}(\overline{x}) = \psi_1(\overline{x})\overline{v}_{1i} + \psi_2(\overline{x})\beta_{1i} + \psi_3(\overline{x})\overline{v}_{2i} + \psi_4(\overline{x})\beta_{2i} \tag{2.35}$$

$$\beta(\overline{x}) = \widehat{\psi}_1(\overline{x})\overline{v}_{1i} + \widehat{\psi}_2(\overline{x})\beta_{1i} + \widehat{\psi}_3(\overline{x})\overline{v}_{2i} + \widehat{\psi}_4(\overline{x})\beta_{2i} \tag{2.36}$$

where $\psi_i(x)$ and $\widehat{\psi}_i(x)$ are given by

$$\psi_i(\overline{x}) = \sum_{m=1}^{4} \Gamma_{mi} e^{r_m \overline{x}} \tag{2.37}$$

$$\widehat{\psi}_i(\overline{x}) = \sum_{m=1}^{4} a_m \Gamma_{mi} e^{r_m \overline{x}} \tag{2.38}$$

in which the constants a_m and Γ_{mi} are given explicitly in Appendix A. It should be noted that the shape functions (2.37) and (2.38) are applicable for the case that r_1, r_2, r_3 and r_4 are all distinct. The shape functions $\psi_i(x)$ and $\widehat{\psi}_i(x)$ for some special cases that (2.31) admits repeated roots are shown in Appendix B and Appendix C.

It is apparent that the shape functions obtained above can be used to generate a trial function that assumes the same function form as the exact buckling shape of the structure. The only difference is that the axial load parameter $\overline{P}_i$ appearing in such shape functions takes arbitrary value and is generally not the same as the buckling load which is unknown a priori. This special trial function, when incorporated with a selected iterative procedure to improve the axial load parameter, can converge to the exact buckling shape. Once the trial function converges to the exact buckling shape, the approximate buckling load estimated by the principle of stationary total potential energy also converges to the exact buckling load.

2.6 Inelastic material model

To model the inelastic flexural buckling, the tangent modulus theory proposed by Engesser (1889) is employed. A model for the stress-strain relationship selected for the present investigation consists of both linear and inelastic regimes described by

$$\varepsilon/\varepsilon_0 = \begin{cases} \sigma/\sigma_0 & ; \ \sigma/\sigma_0 \leq 1 \\ B + (1-B)(\sigma/\sigma_0)^n & ; \ \sigma/\sigma_0 > 1 \end{cases} \tag{2.39}$$

where σ_0 and ε_0 are reference stress and strain and B and n are material constants. It is evident that this constitutive model includes following special cases: (i) a linear stress-strain relation if choosing $B = 0$ and $n = 1$, (ii) a bilinear stress-strain relation if choosing for $B < 0$ and $n = 1$, and a nonlinear stress-strain relation with a continuous tangent modulus at $\sigma/\sigma_0 = 1$ if choosing $B = 1 - 1/n$ and $n > 1$. Plots of the stress-strain relation (2.39) for various exponent n are shown in Figure 2.3(a) for the general case and in Figure 2.3(b) for the case that the tangent modulus is entirely continuous (i.e. $B = 1 - 1/n$). It is evident that the extent of material nonlinearity is governed by the exponent n; more specifically, a material exhibits higher nonlinearity for larger n.
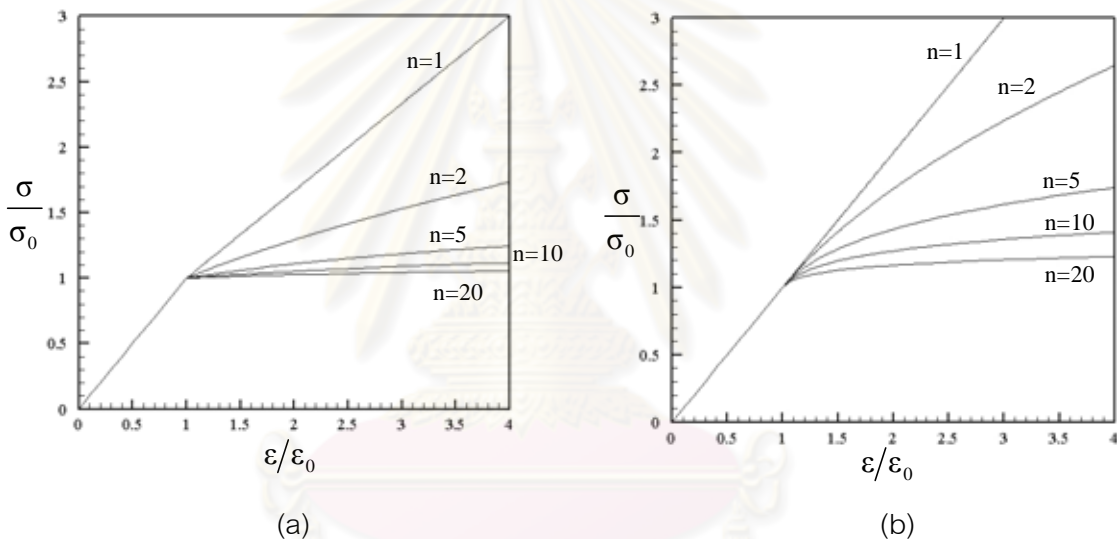
Figure 2.3 Stress-strain relation governed by (2.39): (a) general case with $B = -0.5$ and (b) $B = 1 - 1/n$

The tangent modulus, denoted by E_T, of the stress-stress model (2.39) can readily be obtained by a direct differentiation and the final result is given by

$$E_T = \begin{cases} \sigma_0/\varepsilon_0 & ; \ \sigma/\sigma_0 \leq 1 \\ \dfrac{\sigma_0/\varepsilon_0}{n(1-B)(\sigma/\sigma_0)^{n-1}} & ; \ \sigma/\sigma_0 > 1 \end{cases} \tag{2.39}$$

Plots of the tangent modulus versus the stress level (σ/σ_0) are shown in Figure 2.4 for both the general case and the case that $B = 1 - 1/n$. It is clear that in general, the model

(2.39) yields a finite jump of the tangent modulus at $\sigma/\sigma_0 = 1$ except for the case that $\mathbf{B}$ is chosen equal to $1 - 1/n$.
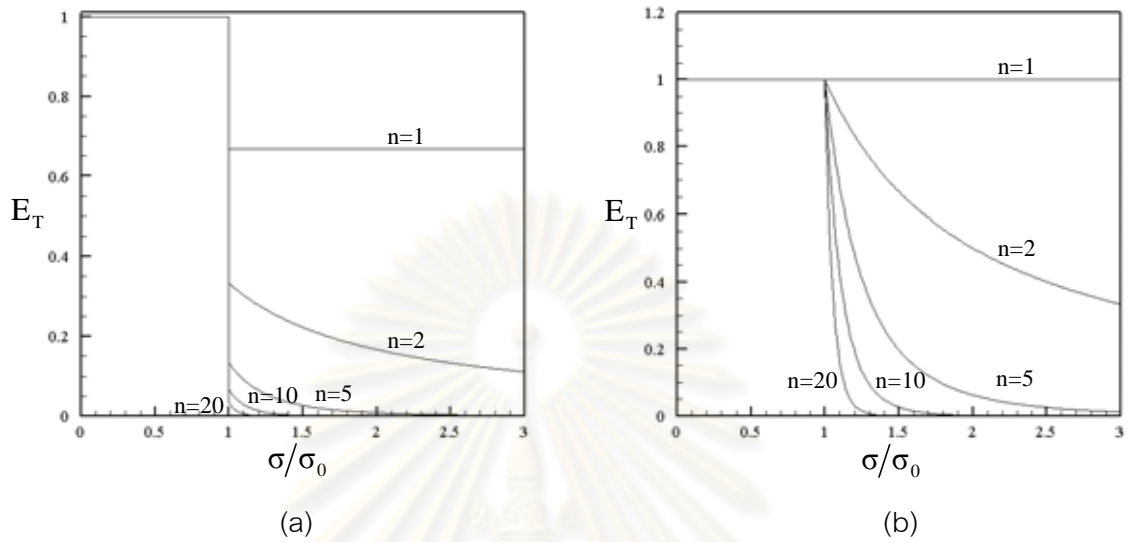
Figure 2.4 Tangent modulus versus stress level (σ/σ_0): (a) general case with $\mathbf{B} = -0.5$ and (b) $\mathbf{B} = 1 - 1/n$

CHAPTER III

SOLUTION METHOD

In this chapter, we briefly summarize numerical procedures employed to approximate the flexural buckling load of structures. Two key steps involved in the implementation are associated with the calculation of the minimum eigenvalue of the eigenvalue problem (2.22) and the iterative algorithm to achieve the converged (exact) buckling shape and buckling load. Before we address those two steps, an explicit expression for all involved elements stiffness matrices is given.

3.1 Element stiffness matrices

Since the shape functions $\psi_i(x)$ and $\widehat{\psi}_i(x)$ are given in terms of exponential functions, all elements stiffness matrices $\mathbf{K}_{bi}$, $\mathbf{K}_{si}$, $\mathbf{K}_{l1i}$, $\mathbf{K}_{l2i}$, and $\mathbf{K}_{gi}$ can readily be obtained in an explicit form via the direct integration. Entries of these matrices are given by

$$\left[\mathbf{K}_{bi}\right]_{mn} = E_i I_i \sum_{j=1}^{4}\sum_{k=1}^{4} a_j a_k r_j r_k \Gamma_{jm}\Gamma_{kn}\left(e^{(r_j+r_k)L}-1\right)\Big/\left(r_j+r_k\right) \tag{3.1}$$

$$\left[\mathbf{K}_{si}\right]_{mn} = \lambda_i G_i A_i \sum_{j=1}^{4}\sum_{k=1}^{4} (r_j-a_j)(r_k-a_k)\Gamma_{jm}\Gamma_{kn}\left(e^{(r_j+r_k)L}-1\right)\Big/\left(r_j+r_k\right) \tag{3.2}$$

$$\left[\mathbf{K}_{l1i}\right]_{mn} = k_{1i}\sum_{j=1}^{4}\sum_{k=1}^{4}\Gamma_{jm}\Gamma_{kn}\left(e^{(r_j+r_k)L}-1\right)\Big/\left(r_j+r_k\right) \tag{3.3}$$

$$\left[\mathbf{K}_{l2i}\right]_{mn} = k_{2i}\sum_{j=1}^{4}\sum_{k=1}^{4} r_j r_k \Gamma_{jm}\Gamma_{kn}\left(e^{(r_j+r_k)L}-1\right)\Big/\left(r_j+r_k\right) \tag{3.4}$$

$$\left[\mathbf{K}_{gi}\right]_{mn} = P_i\sum_{j=1}^{4}\sum_{k=1}^{4} r_j r_k \Gamma_{jm}\Gamma_{kn}\left(e^{(r_j+r_k)L}-1\right)\Big/\left(r_j+r_k\right) \tag{3.5}$$

It is worth noting that while roots of the characteristic equation (i.e. r_1, r_2, r_3 and r_4) can be complex numbers, it can readily be verified that all entries of the matrices $\mathbf{K}_{bi}$, $\mathbf{K}_{si}$, $\mathbf{K}_{l1i}$, $\mathbf{K}_{l2i}$, and $\mathbf{K}_{gi}$ shown above are real numbers. The arithmetic involving complex numbers can readily be treated using any standard computer languages. Explicit results for other special cases are shown in Appendix B and Appendix C.

3.2 Determination of minimum eigenvalue and corresponding eigenvector

In this investigation, a numerical technique based on a power method supplemented by the Rayleigh quotient scheme (e.g. Hamming, 1987; Chapra and Canale, 1990; and Notay, 2001) is adopted to estimate the minimum eigenvalue of the eigenvalue problem (2.22). Key steps for this iterative technique can be summarized as follows:

(i)   Start the iteration by choosing an initial guess vector $\mathbf{v}_k$

(ii)   Construct a vector $\mathbf{b}_k$ from a simple matrix-vector multiplication

$$\mathbf{b}_k = \hat{\mathcal{K}}_g \mathbf{v}_k \tag{3.6}$$

(iii)   Obtain the update vector $\mathbf{v}_{k+1}$ by solving a system of linear equations

$$\left(\hat{\mathcal{K}}_b + \hat{\mathcal{K}}_s + \hat{\mathcal{K}}_{11} + \hat{\mathcal{K}}_{12} \right) \mathbf{v}_k = \mathbf{b}_k \tag{3.7}$$

using LU decomposition

(iv)   Estimate the minimum eigenvalue, P_{0k}, by forming the Rayleigh quotient

$$P_{0k} = \frac{\mathbf{v}_{k+1}^T \left(\hat{\mathcal{K}}_b + \hat{\mathcal{K}}_s + \hat{\mathcal{K}}_{11} + \hat{\mathcal{K}}_{12} \right) \mathbf{v}_{k+1}}{\mathbf{v}_{k+1}^T \hat{\mathcal{K}}_g \mathbf{v}_{k+1}} \tag{3.8}$$

(v)   Check convergence of the estimated eigenvalue from following criteria

$$\left| \frac{P_{0k} - P_{0k-1}}{P_{0k-1}} \right| < \varepsilon \tag{3.9}$$

where ε is a specified tolerance (use 10^{-9} in the present study). If the above criterion is satisfied, the iterative is terminated and the minimum eigenvalue is obtained; otherwise, return to step (II).

A flowchart demonstrating the iterative procedure for the power method and the Rayleigh quotient is shown in Figure 3.1.
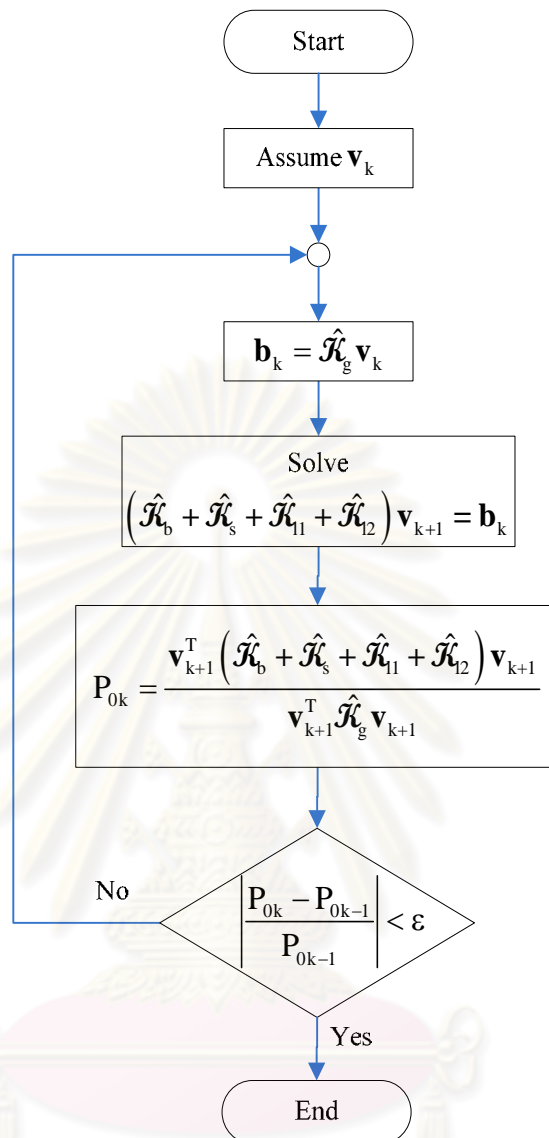
Figure 3.1 Flowchart demonstrating the power method and Rayleigh quotient for determining the minimum eigenvalue

3.3 Iterative procedure to improve buckling load

It is apparent from section 2.5 that special basis functions utilized in the approximation allow automatic adaptivity in the sense that the involved axial load parameter $\overline{P}_i$ can be varied in an arbitrary manner. In addition, based on a means that these functions were derived, they can form a space of trial functions that contain the exact buckling shape if the axial load P_i is chosen to be identical to the buckling load of the member. By using these two positive features, proper iterative schemes can be

developed to improve the approximate buckling shape and, at the same time, enhance the accuracy of the buckling load estimation. In this study, we propose an iterative procedure based on a following conjecture: shape functions based on the axial load parameter $\overline{P}_i$ computed from the previous estimated buckling load provides a better approximation of the buckling shape. While the validity of this conjecture has not been confirmed mathematically, the iterative procedure implemented in this study by following this idea has been found compromising and robust (see results and discussion in Chapter 4).

The iterative procedure begins first with guessing the buckling load of all members and using this information to compute the axial load parameter $\overline{P}_i$ for each member. The shape functions based on this set of axial load parameters (i.e. those given by equations (2.37) and (2.38)) are then used in the Rayleigh-Ritz approximation for the first estimation of the buckling load. Based on above conjecture, the estimated buckling load can now be used to update the axial load parameter for each member and the shape functions based on this new axial load parameter should improve the estimation of the buckling load in the next iteration. Due to the anticipated improvement of the buckling load and buckling shape estimation in any iteration, the scheme should eventually yield a converged result comparable to the exact solution.

To update of the axial parameter $\overline{P}_i = P_i L_i^2 / E_i I_i$, it is also required to replace the modulus E_i by the tangent modulus E_{Ti}. To estimate the new tangent modulus for the next iteration, we assume that the effective length factor of each member is identical to that for the current iteration and the E_{Ti} can be obtained from (2.39) by setting $E_T = E_{Ti}$ and $\sigma = \pi^2 E_{Ti} I_i / (K_i L_i)^2 A_i$ where A_i is the cross-sectional area of the ith member and K_i is the effective length factor of the ith member obtained in the current iteration. The explicit expression for E_{Ti} is given by

$$E_{Ti} = \begin{cases} \sigma_0/\varepsilon_0 & ; \ \sigma/\sigma_0 \leq 1 \\ \sqrt[n]{\dfrac{\sigma_0/\varepsilon_0}{n(1-B)\left(\dfrac{\pi^2 I_i}{\sigma_0 A_i (K_i L_i)^2}\right)^{n-1}}} & ; \ \sigma/\sigma_0 > 1 \end{cases} \tag{3.10}$$

Two different iterative procedures to obtain the converged buckling load are proposed in the current study as indicated in Figure 3.2 and Figure 3.3. The detailed descriptions for each procedure are given below.

First iterative procedure:

(i) Input essential data, e.g. structure geometry, member and material properties, axial load factor, etc.

(ii) Set $j = 1$ and $N = 1$, where j and N are the iteration number for updating the tangent modulus and the number of adaptive steps, and then guess the axial load parameter for all members

(iii) Compute element stiffness matrices $\mathbf{K}_{bi}$, $\mathbf{K}_{si}$, $\mathbf{K}_{l1i}$, $\mathbf{K}_{l2i}$, and $\hat{\mathbf{K}}_{gi}$ for all members

(iv) Assemble element stiffness matrices to obtain the unconstrained global stiffness matrices $\mathcal{K}_b$, $\mathcal{K}_s$, $\mathcal{K}_{l1}$, $\mathcal{K}_{l2}$ and $\mathcal{K}_g$

(v) Remove rows and columns of $\mathcal{K}_b$, $\mathcal{K}_s$, $\mathcal{K}_{l1}$, $\mathcal{K}_{l2}$ and $\mathcal{K}_g$ associated with degrees of freedom where the essential boundary conditions are prescribed to obtain $\hat{\mathcal{K}}_b$, $\hat{\mathcal{K}}_s$, $\hat{\mathcal{K}}_{l1}$, $\hat{\mathcal{K}}_{l2}$ and $\hat{\mathcal{K}}_g$

(vi) Solve the eigenvalue problem (2.22) to obtain the minimum eigenvalue P_0^N by using the iterative procedure shown in Figure 3.1

(vii) Determine the approximate buckling load for each member from $P_{N+1}^{(i)} = \alpha_i P_0^N$

(viii) Check convergence of the approximate buckling load using the criteria $\left| \dfrac{P_0^N - P_0^{N-1}}{P_0^N} \right| < \varepsilon$ where ε is a specified tolerance (use 10^{-6} in the present study). If the convergence is not achieved, then update the axial load parameter $P_{N+1}^{(i)} L^2 / E_{Ti}^j I_i$ and return to step (iii); otherwise, go to step (ix)

(ix) Obtain the converged buckling load for each member $P_{N+1}^{(i)}$ and use $P_{N+1}^{(i)}$ to calculate the tangent modulus for the next iteration E_{Ti}^{j+1} from equation (3.10)

(x) Check convergence of the tangent modulus using the criteria
$\left| \dfrac{E_T^j - E_T^{j+1}}{E_T^j} \right| < \varepsilon$ where ε is specified tolerance (use 10^{-6} in the present
study). If the convergence is achieved, obtain the final approximate
buckling load for each member and terminate the procedure;
otherwise, update the new axial load parameter for all members using
the new tangent modulus obtained from step (ix) and return to step (iii).

Second iterative procedure:

(i) Input essential data, e.g. structure geometry, member and material
properties, axial load factor, etc.

(ii) Set N = 1, where N is the number of adaptive steps, and then guess the
axial load parameter for all members

(iii) Compute element stiffness matrices $\mathbf{K}_{bi}$, $\mathbf{K}_{si}$, $\mathbf{K}_{l1i}$, $\mathbf{K}_{l2i}$, and $\hat{\mathbf{K}}_{gi}$ for
all members

(iv) Assemble element stiffness matrices to obtain the unconstrained global
stiffness matrices $\mathcal{K}_b$, $\mathcal{K}_s$, $\mathcal{K}_{l1}$, $\mathcal{K}_{l2}$ and $\mathcal{K}_g$

(v) Remove rows and columns of $\mathcal{K}_b$, $\mathcal{K}_s$, $\mathcal{K}_{l1}$, $\mathcal{K}_{l2}$ and $\mathcal{K}_g$ associated with
degrees of freedom where the essential boundary conditions are
prescribed to obtain $\hat{\mathcal{K}}_b$, $\hat{\mathcal{K}}_s$, $\hat{\mathcal{K}}_{l1}$, $\hat{\mathcal{K}}_{l2}$ and $\hat{\mathcal{K}}_g$

(vi) Solve the eigenvalue problem (2.22) to obtain the minimum eigenvalue
P_0^N by using the iterative procedure shown in Figure 3.1

(vii) Determine the approximate buckling load for each member from
$P_{N+1}^{(i)} = \alpha_i P_0^N$ and use $P_{N+1}^{(i)}$ to calculate the tangent modulus for the next
iteration E_{Ti}^{N+1} from equation (3.10)

(viii) Check convergence of the approximate buckling load using the criteria
$\left| \dfrac{P_0^N - P_0^{N-1}}{P_0^N} \right| < \varepsilon$ and convergence of the tangent modulus using the
criteria $\left| \dfrac{E_{Ti}^N - E_{Ti}^{N+1}}{E_{Ti}^N} \right| < \varepsilon$ where ε is a specified tolerance (use 10^{-6} in the
present study). If the convergence is not achieved, then update the

axial load parameter $P_{N+1}^{(i)} L^2 / E_{Ti}^{N+1} I_i$ and return to step (iii); otherwise, go to step (ix)

(ix) Obtain the converged buckling load for each member $P_{N+1}^{(i)}$ and show results

It should be noted that the key difference between the two iterative procedures is associated with the update of the tangent modulus for each member. For the first scheme, the tangent modulus for each member (E_{Ti}^{j}) is estimated before enter the loop for updating the adaptive shape functions using the information of the previous converged buckling load and this tangent modulus is held constant for all iterations in the inside loop. For the second scheme, the tangent modulus and the adaptive shape functions are updated simultaneously within a single loop for iterations. From extensive numerical experiments, both schemes yielded the same converged results but the second procedure requires less computational time.

We also remark that to accelerate the convergence rate of the minimum eigenvalue computation, an initial guess of the eigenvector in the Nth adaptive step is chosen from the converged eigenvector obtained in the $(N-1)^{th}$ adaptive step. The number of adaptive steps required for obtaining the converged buckling load for a specified tolerance and the number of iterations required in the computation of the minimum eigenvalue in each adaptive step are thoroughly investigated to demonstrate the computational efficiency of the developed technique.
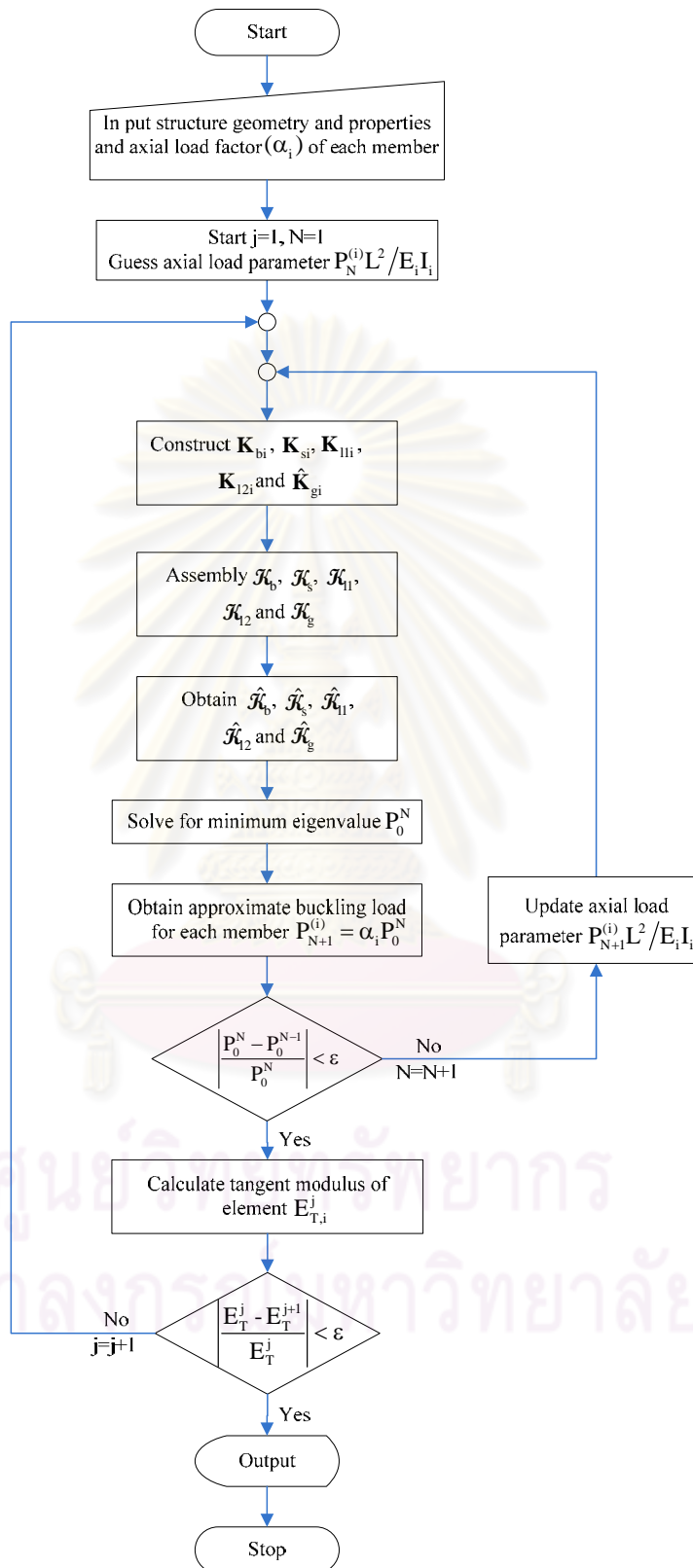
Figure 3.2 Flowchart demonstrating iterative procedure to obtain converged buckling load of first numerical scheme
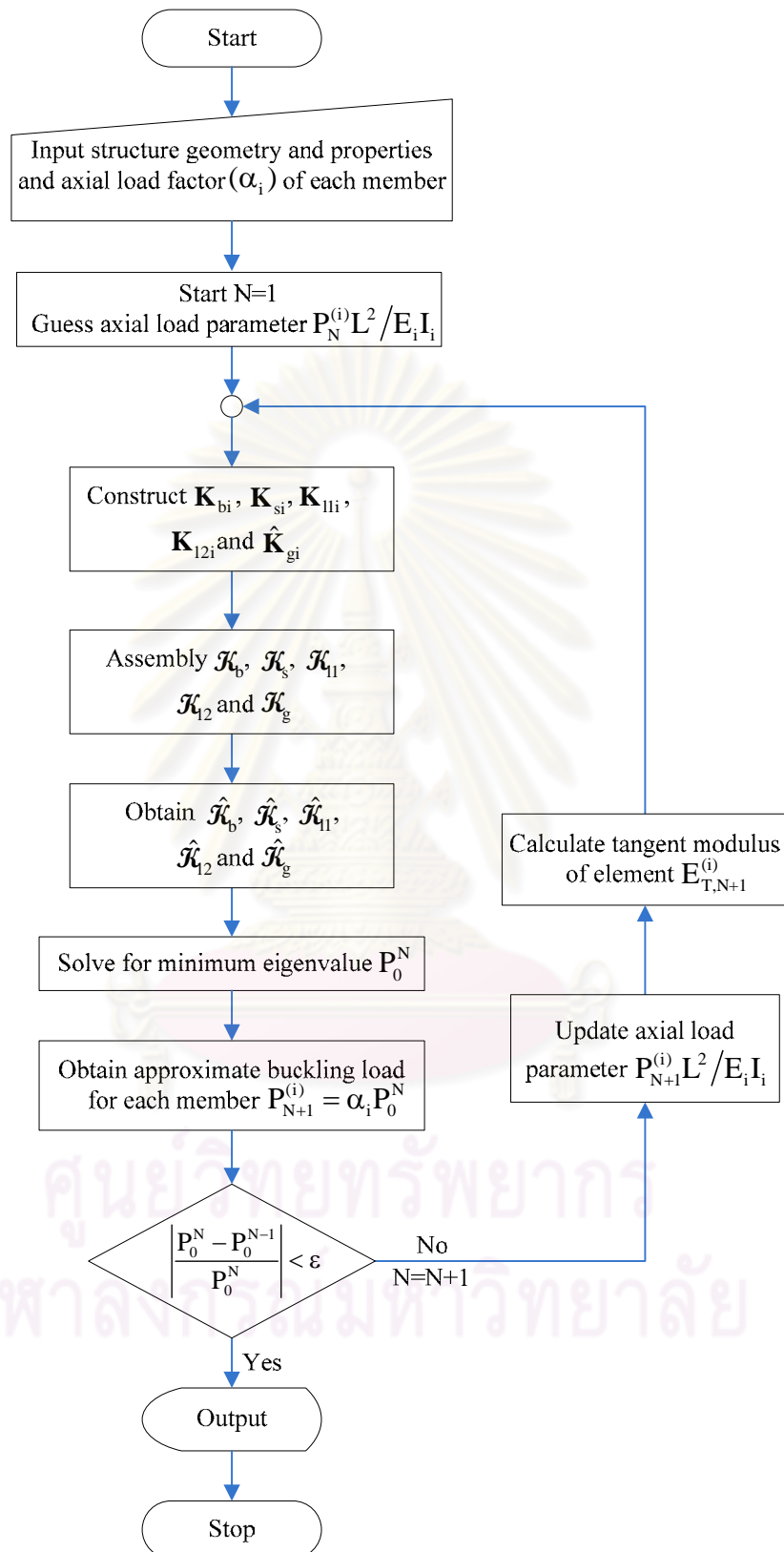
Figure 3.3 Flowchart demonstrating iterative procedure to obtain converged buckling load of second numerical scheme

CHAPTER IV

NUMERICAL RESULTS

In this chapter, we demonstrate the accuracy and convergence behavior of approximate solutions and computational efficiency of the proposed numerical procedure in the flexural buckling analysis of various structures, and a set of selected results is reported and discussed. To verify both the formulation and numerical implementation of the current technique, several examples whose analytical solution exists are first considered in numerical experiments. Once the method is tested, it is then applied to analyze more complex structures to demonstrate their capability. The number of adaptive steps (N) and the number of iterations required in the computation of the minimum eigenvalue in each iterative step ($\tilde{n}$) are also reported to indicate the computational cost.

4.1 Single column with various end conditions

Consider a perfectly straight column of length L, Young modulus E, moment of inertia I, and subjected to axial load P and various end conditions as shown in Figure 4.1. In the analysis, only one member is employed in the discretization and we choose the reference stress σ_0 = 35143581 kg/m^2, the reference strain ε_0 = 0.00172405, I = 0.00013333 m^4, A = 0.04 m^2 and L = 1 m. The percent error of the approximation ($|P_{current}-P_{exact}|/ P_{exact}*100$), the number of adaptive steps (N) and iterations required for eigen computation ($\tilde{n}$) are reported in Table 4.1-Table 4.6. Note that the exact elastic and inelastic buckling loads (P_{exact}) are given by $\pi^2EI / (KL)^2$ and $\pi^2E_TI / (KL)^2$, respectively, where the effective length factor (K) for each end condition can be readily found (e.g. Timoshenko and Gere, 1961; Chajes, 1974) and the exact tangent modulus can be computed from equation (3.10). It is evident that the numerical solutions are in excellent agreement with the analytical solutions. Only few adaptive steps are required to achieve the converged buckling load. In addition, by using the converged eigenvector from the previous adaptive step as an initial guess in the current step, computation of the minimum eigenvalue also requires only a few iterations.
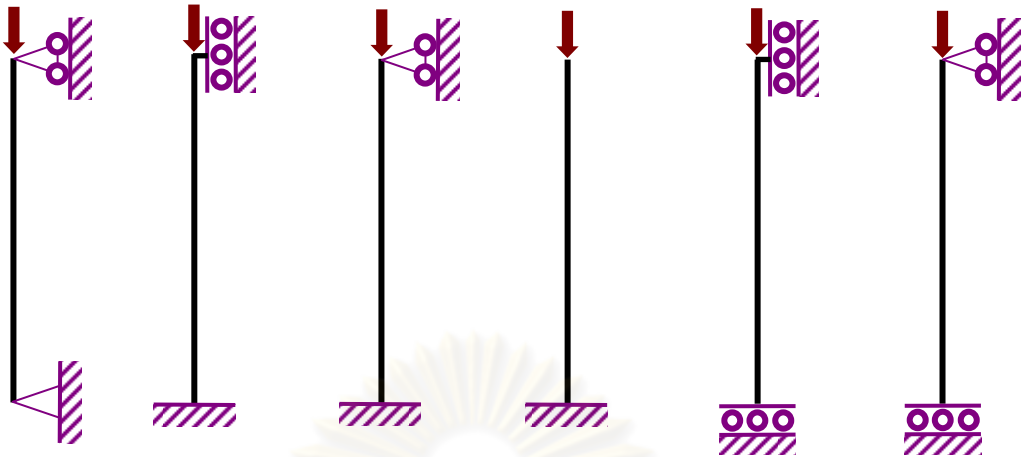
Figure 4.1 Schematic of single column subjected to (a) pined-pined conditions, (b) fixed-fixed conditions, (c) fixed-pinned conditions, (d) fixed-free conditions, (e) guided-fixed conditions, and (f) guided-pinned conditions

Table 4.1 Percent error of the approximation ($|P_{current}-P_{exact}|/ P_{exact}*100$) and number of adaptive steps and required iterations for minimum eigenvalue calculations for column with pinned-pinned condition

N	Elastic buckling	Inelastic Buckling		
		n = 2, B = 0.5	n = 5, B = 0.8	n = 10, B = 0.9
	Error (%), $(\tilde{n})$	Error (%), $(\tilde{n})$	Error (%), $(\tilde{n})$	Error (%), $(\tilde{n})$
1	17.694560, (7)	414.339097, (8)	1145.255513, (8)	1572.327132, (9)
2	0.802960, (2)	7.098078, (2)	11.515300, (2)	12.945235, (2)
3	0.001614, (2)	0.399663, (2)	0.636157, (2)	0.715591, (2)
4	0.000000, (2)	0.000816, (2)	0.001291, (2)	0.001452, (2)
5	0.000000, (2)	0.000000, (2)	0.000000, (2)	0.000000, (2)
6	-	0.000000, (2)	0.000000, (2)	0.000000, (2)

Table 4.2 Percent error of the approximation ($|P_{current} - P_{exact}|/P_{exact}*100$) and number of adaptive steps and required iterations for minimum eigenvalue calculations for column with fixed-fixed condition

N	Elastic buckling	Inelastic Buckling		
		n = 2, B = 0.5	n = 5, B = 0.8	n = 10, B = 0.9
	Error (%), (ñ)	Error (%), (ñ)	Error (%), (ñ)	Error (%), (ñ)
1	1.088759, (6)	784.683240, (9)	3147.835950, (9)	4910.289796, (9)
2	0.000194, (2)	0.624544, (2)	0.997551, (2)	1.121576, (2)
3	0.000000, (2)	0.000130, (2)	0.000208, (2)	0.000234, (2)
4	0.000000, (2)	0.000000, (2)	0.000000, (2)	0.000000, (2)
5	-	0.000000, (2)	0.000000, (2)	0.000000, (2)

Table 4.3 Percent error of the approximation ($|P_{current} - P_{exact}|/P_{exact}*100$) and number of adaptive steps and required iterations for minimum eigenvalue calculations for column with fixed-pinned condition

N	Elastic buckling	Inelastic Buckling		
		n = 2, B = 0.5	n = 5, B = 0.8	n = 10, B = 0.9
	Error (%), (ñ)	Error (%), (ñ)	Error (%), (ñ)	Error (%), (ñ)
1	44.735537, (2)	804.615214, (2)	2614.932711, (2)	3816.580498, (2)
2	18.421494, (2)	1.546228, (2)	11.901119, (2)	15.098986, (2)
3	2.776489, (2)	5.559987, (2)	10.226254, (2)	11.731389, (2)
4	0.058582, (2)	1.308366, (2)	2.109775, (2)	2.377495, (2)
5	0.000026, (2)	0.029551, (2)	0.046815, (2)	0.052669, (2)
6	0.000000, (2)	0.000013, (2)	0.000021, (2)	0.000023, (2)
7	-	0.000000, (2)	0.000000, (2)	0.000000, (2)

Table 4.4 Percent error of the approximation ($|P_{current} - P_{exact}|/ P_{exact} * 100$) and number of adaptive steps and required iterations for minimum eigenvalue calculations for column with fixed-free condition

N	Elastic buckling	Inelastic Buckling		
	Error (%), (ñ)	n = 2, B = 0.5	n = 5, B = 0.8	n = 10, B = 0.9
		Error (%), (ñ)	Error (%), (ñ)	Error (%), (ñ)
1	0.277732, (5)	119.032773, (6)	249.992397, (6)	309.180919, (6)
2	0.000006, (2)	0.140960, (3)	0.221625, (3)	0.249295, (3)
3	0.000000, (2)	0.000003, (2)	0.000005, (2)	0.000006, (2)
4	-	0.000000, (2)	0.000000, (2)	0.000000, (2)

Table 4.5 Percent error of the approximation ($|P_{current} - P_{exact}|/ P_{exact} * 100$) and number of adaptive steps and required iterations for minimum eigenvalue calculations for column with guided-fixed condition

N	Elastic buckling	Inelastic Buckling		
	Error (%), (ñ)	n = 2, B = 0.5	n = 5, B = 0.8	n = 10, B = 0.9
		Error (%), (ñ)	Error (%), (ñ)	Error (%), (ñ)
1	1.088754, (2)	341.587385, (2)	969.559490, (2)	1336.374571, (2)
2	0.000194, (2)	0.539779, (2)	0.862363, (2)	0.969658, (2)
3	0.000000, (2)	0.000097, (2)	0.000155, (2)	0.000174, (2)
4	0.000000, (2)	0.000000, (2)	0.000000, (2)	0.000000, (2)
5	-	-	0.000000, (2)	0.000000, (2)

Table 4.6 Percent error of the approximation ($|P_{current}-P_{exact}|/ P_{exact}*100$) and number of adaptive steps and required iterations for minimum eigenvalue calculations for column with guided-pinned condition

N	Elastic buckling	Inelastic Buckling		
		n = 2, B = 0.5	n = 5, B = 0.8	n = 10, B = 0.9
	Error (%), (ñ)	Error (%), (ñ)	Error (%), (ñ)	Error (%), (ñ)
1	0.277732, (5)	119.032773, (6)	249.992397, (6)	309.180919, (6)
2	0.000006, (2)	0.140960, (3)	0.221625, (3)	0.249295, (3)
3	0.000000, (2)	0.000003, (2)	0.000005, (2)	0.000006, (2)
4	-	0.000000, (2)	0.000000, (2)	0.000000, (2)

4.2 Rigid frame and equivalent model with rotational spring

Next, consider a rigid frame consisting of a column and two beams as shown schematically in Figure 4.2(a). Length of the column, the left beam and the right beam are given by L, ρL and λL, respectively, where ρ and λ are length ratios; the flexural rigidity of the column, the left beam and the right beam are given by EI, γEI and μEI, respectively, where γ and μ are constants indicating the flexural rigidity ratio; and the vertical load P is applied to the top of column. To demonstrate the capability of the current technique to treat a concentrated rotational spring, we also consider two other equivalent models in the analysis for the buckling load of the column: one obtained by replacing the right beam by an elastic rotational spring with stiffness $3\mu EI/\lambda L$ at the top of the column as shown in Figure 4.2(b) and the other obtained by replacing both beams by an elastic rotational spring with stiffness $3\mu EI/\lambda L + 3\gamma EI/\rho L$ at the top of the column as shown in Figure 4.2(c). In the analysis, the three structural models are discretized using only 3, 2 and 1 elements, respectively. Computed elastic buckling loads, normalized such that $\hat{P}_{current}=P_{current}/(\pi^2 EI/L^2)$, are reported in Table 4.7 along with the normalized exact solution $\hat{P}_{exact}=P_{exact}/(\pi^2 EI/L^2)$ obtained from directly solving the differential equation and exact eigenvalue problem for several values of {γ, ρ, μ, λ}.

In the inelastic buckling analysis, σ_0 = 24607437 kg/m^2, ε_0 = 0.00346535, I = 0.00636173 m^4, A = 0.28274 m^2 and L = 1 m are chosen. The normalized inelastic buckling loads are reported in Table 4.8 and Table 4.9 compared with the normalized exact solution for n = 4, B = 0.75 and n = 8, B = 0.875, respectively. The number of adaptive steps and the total number of iterations in the eigenvalue computation are also reported. As is clearly indicated for both elastic buckling and inelastic buckling, approximate solutions are comparable to the exact solution for all three models. In addition, the number of adaptive steps required to achieve the converged solutions for both elastic and inelastic cases is relatively few; in particular, the number of adaptive steps for the inelastic case is larger than that for the elastic case.
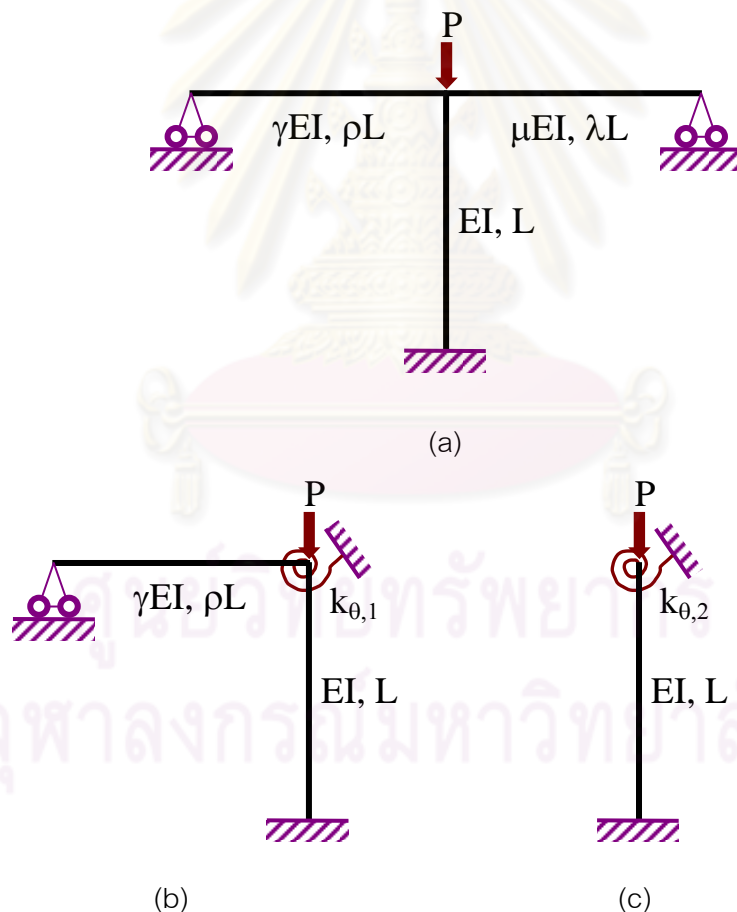

Figure 4.2 (a) Schematic of rigid frame subjected to vertical load P at top of column, (b) equivalent model obtained by replacing right beam by elastic rotational spring at top of column, and (c) equivalent model obtained by replacing left and right beams by elastic rotational spring at top of column

Table 4.7 Normalized computed elastic buckling loads of rigid frame using three different models compared with normalized exact solution

					Model (a)	Model (b)	Model (c)
γ	ρ	μ	λ	$\hat{P}_{exact}$	$\hat{P}_{current}$, $(N, \sum \tilde{n})$	$\hat{P}_{current}$, $(N, \sum \tilde{n})$	$\hat{P}_{current}$, $(N, \sum \tilde{n})$
1	1	1	1	0.747665	0.747665 (3,12)	0.747665 (3,12)	0.747665 (3,12)
3	1	1	1	0.854549	0.854549 (3,12)	0.854549 (3,10)	0.854549 (3,10)
1	3	1	1	0.669441	0.669441 (3,12)	0.669441 (3,13)	0.669441 (3,12)
1	1	3	1	0.854549	0.854549 (3,12)	0.854549 (3,10)	0.854549 (3,10)
1	1	1	3	0.669441	0.669441 (3,12)	0.669441 (3,13)	0.669441 (3,12)
1	1	1	0.1	0.942198	0.942198 (4,12)	0.942198 (4,12)	0.942198 (4,12)
1	0.1	1	0.1	0.967510	0.967510 (4,11)	0.967510 (4,11)	0.967510 (4,11)

Table 4.8 Normalized computed inelastic buckling loads of rigid frame using three different models compared with normalized exact solution for n = 4 and B = 0.75

					Model (a)	Model (b)	Model (c)
γ	ρ	μ	λ	$\hat{P}_{exact}$	$\hat{P}_{current}$, $(N, \sum \tilde{n})$	$\hat{P}_{current}$, $(N, \sum \tilde{n})$	$\hat{P}_{current}$, $(N, \sum \tilde{n})$
1	1	1	1	0.043988	0.043988 (7, 21)	0.043988 (7, 21)	0.043988 (7, 21)
3	1	1	1	0.044070	0.044070 (6,19)	0.044070 (6,19)	0.044070 (6,19)
1	3	1	1	0.043906	0.043906 (7, 21)	0.043906 (7, 21)	0.043906 (7, 21)
1	1	3	1	0.044070	0.044070 (6,19)	0.044070 (6,19)	0.044070 (6,19)
1	1	1	3	0.043906	0.043906 (7, 21)	0.043906 (7, 21)	0.043906 (7, 21)
1	1	1	0.1	0.044122	0.044122 (5,14)	0.044122 (5,14)	0.044122 (5,14)
1	0.1	1	0.1	0.044136	0.044136 (5,14)	0.044136 (5,14)	0.044136 (5,14)

4.3 Simply-support column braced by translational spring at its mid-span

Next, consider a simply-supported column of length 2L and flexural rigidity EI and being braced against the lateral movement at its mid-span by an elastic translational spring stiffness k as shown in Figure 4.3(a). This problem was solved analytically and reported by Timoshenko and Gere (1961). It was demonstrated that the buckling switches from a single curvature mode to a double curvature mode (similar to

Table 4.9 Normalized computed inelastic buckling loads of rigid frame using three different models compared with normalized exact solution for n = 8 and B = 0.875

γ	ρ	μ	λ	$\hat{P}_{exact}$	Model (a) $\hat{P}_{current}$, (N, $\sum \tilde{n}$)	Model (b) $\hat{P}_{current}$, (N, $\sum \tilde{n}$)	Model (c) $\hat{P}_{current}$, (N, $\sum \tilde{n}$)
1	1	1	1	0.026220	0.026220 (6, 20)	0.026220 (6, 20)	0.026220 (6, 20)
3	1	1	1	0.026234	0.026234 (6,18)	0.026234 (6,18)	0.026234 (6,18)
1	3	1	1	0.026205	0.026205 (7, 21)	0.026205 (7, 21)	0.026205 (7, 21)
1	1	3	1	0.026234	0.026234 (6,18)	0.026234 (6,18)	0.026234 (6,18)
1	1	1	3	0.026205	0.026205 (7, 21)	0.026205 (7, 21)	0.026205 (7, 21)
1	1	1	0.1	0.026243	0.026243 (5,14)	0.026243 (5,14)	0.026243 (5,14)
1	0.1	1	0.1	0.026246	0.026246 (5,14)	0.026246 (5,14)	0.026246 (5,14)
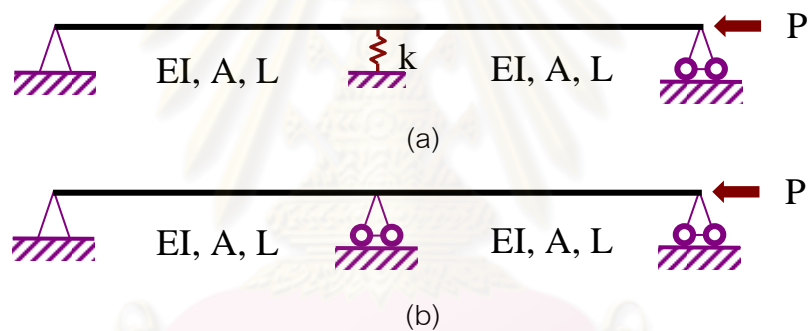
Figure 4.3 (a) Simply-supported column braced against lateral movement at its mid-span by translational spring and (b) two-span column with equal length

the buckling mode of a column shown in Figure 4.3(b)) when the spring stiffness k reaches the value $16\pi^2 EI/(2L)^3$. In the analysis, the column is discretized into 2 equal elements and numerical results are shown in Table 4.10 for various values of normalized spring stiffness $\overline{k} = k / (\pi^2 EI/(2L)^3)$ and in Figure 4.4 for the entire range of $\overline{k}$. As anticipated, converged buckling loads obtained from the current technique for various values of k are identical to the exact solution and the number of adaptive steps required is relatively low. In addition, the technique requires no additional treatment in order to accurately capture the mode switching. It should be pointed out, however, that when the

spring stiffness k close to the critical value (i.e. $16\pi^2EI/(2L)^3$), it is required the larger number of the iterations to compute the minimum eigenvalue.

Table 4.10 Normalized elastic buckling load of simply-supported column braced at its mid-span by translational spring with stiffness k. The number of adaptive steps (N) and the total number of iterations for eigenvalue computation ($\sum \tilde{n}$) are also reported

$\overline{k}$	N	$\sum \tilde{n}$	$\dfrac{P_{current}}{\pi^2 EI/(2L)^2}$	$\dfrac{P_{exact}}{\pi^2 EI/(2L)^2}$
0	3	12	1.000000	1.000000
4	4	15	1.798972	1.798972
8	4	24	2.570652	2.570652
12	4	37	3.307505	3.307505
16	4	55	4.000000	4.000000
20	5	183	4.000000	4.000000
40	5	27	4.000000	4.000000
100	5	21	4.000000	4.000000
∞	5	17	4.000000	4.000000

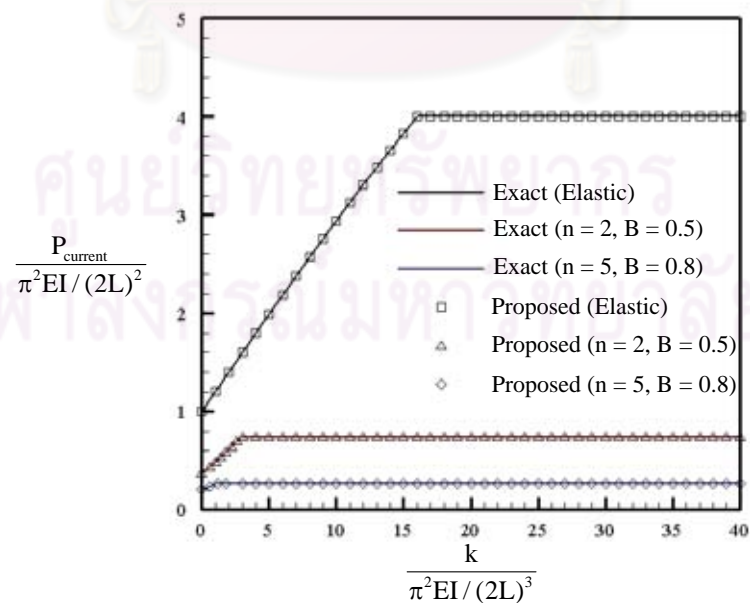Figure 4.4 Normalized buckling load for simply-supported column braced at its mid-span by translational spring versus the normalized spring stiffness

Next, the inelastic buckling of the same structure is investigated. In the analysis, the reference stress σ_0 = 2812278.5 kg/m^2, the reference strain ε_0 = 0.00110938, I = 0.00013333 m^4, A = 0.04 m^2 and L = 1 m are employed. Numerical and exact solutions are presented in Table 4.11 for various values of $\bar{k}$ and in Figure 4.4 for the entire range of $\bar{k}$. In addition, the buckling shapes of the column for both elastic and inelastic cases are also reported in Figure 4.5 for certain values of $\bar{k}$, n and B. It is evident that for a small value of $\bar{k}$ (buckling in a single curvature mode), the buckling shapes for elastic and inelastic cases exhibit slight difference in the middle region of the column whereas, for a large value of $\bar{k}$ (buckling in a double curvature mode), the buckling shapes for all cases are identical.

Table 4.11 Normalized inelastic buckling load of simply-supported column braced at its mid-span by translational spring with stiffness k. The number of adaptive steps (N) and the total number of iterations for eigenvalue computation ($\sum \tilde{n}$) are also reported

$\bar{k}$	n = 2, B = 0.5				n = 5, B = 0.8			
	N	$\sum \tilde{n}$	$\dfrac{P_{current}}{\pi^2 EI/(2L)^2}$	$\dfrac{P_{Exact}}{\pi^2 EI/(2L)^2}$	N	$\sum \tilde{n}$	$\dfrac{P_{current}}{\pi^2 EI/(2L)^2}$	$\dfrac{P_{Exact}}{\pi^2 EI/(2L)^2}$
0	4	14	0.367266	0.367266	4	15	0.201358	0.201358
1	12	40	0.480689	0.480689	26	99	0.261131	0.261131
1.5	14	47	0.544713	0.544713	9	113	0.265694	0.265694
2	15	54	0.611299	0.611299	7	89	0.265694	0.265694
2.5	16	62	0.678074	0.678074	7	67	0.265694	0.265694
3	16	72	0.734532	0.734532	7	61	0.265694	0.265694
5	7	85	0.734532	0.734532	7	58	0.265694	0.265694
10	6	57	0.734532	0.734532	6	55	0.265694	0.265694
∞	6	20	0.734532	0.734532	6	26	0.265694	0.265694

4.4 Column resting on elastic foundation

Consider, next, the flexural buckling of a single column resting on an elastic two-parameter foundation as shown in Figure 4.6. This fourth example is chosen

to further verify the developed technique for the case that both the shear deformation and an elastic foundation are included in the mathematical model. For this particular problem, the exact buckling load is available for a column with the pinned-pinned end condition whereas the benchmark numerical solutions were presented by Seemapholkul (2000) for a column with both pinned-fixed and fixed-fixed end conditions.
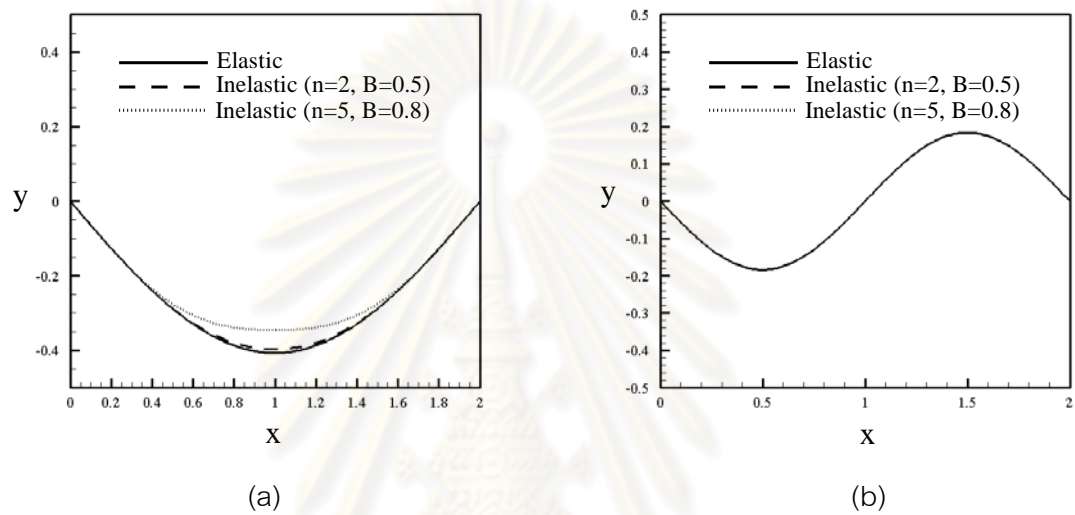

Figure 4.5 Buckling shape of simply-supported column braced at its mid-span by translational spring versus the normalized spring stiffness: (a) $\overline{k} = 1$ and (b) $\overline{k} = 20$
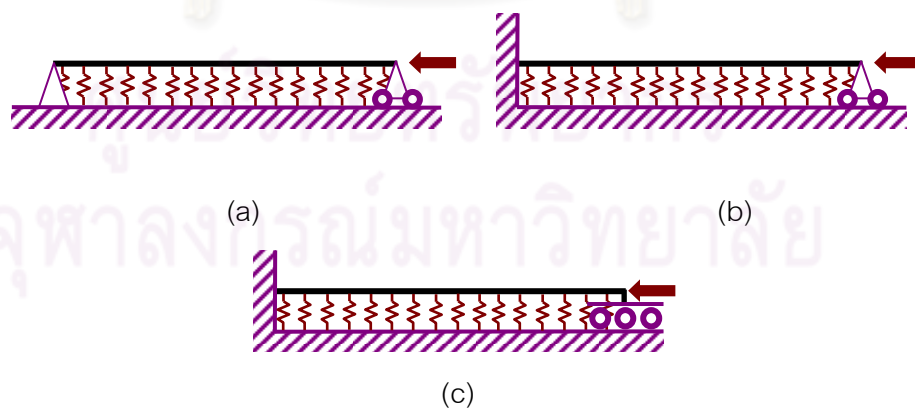

Figure 4.6 Schematic of column resting on an elastic two-parameter foundation with (a) pinned-pinned end condition, (b) pinned-fixed end condition, and (c) fixed-fixed end condition

In the modeling, only one element is used in the discretization for the pinned-pinned and fixed-pinned columns whereas 2 elements are utilized for the fixed-fixed column. In numerical experiments, essential parameters are chosen to be identical to those used by Seemapholkul (2000), for instance, E = 29,000 ksi, L/R = 100 in, I = 719 in^4, A = 32.9 in^2 and G = 11,600 ksi. Numerical results for the buckling load obtained for the three end conditions are reported in Table 4.12. It is evident that the converged buckling load for the pinned-pinned column predicted by the current technique is identical to the exact solution whereas those for the fixed-pinned and fixed-fixed columns show very good agreement with the benchmark numerical solutions. Again, only few adaptive steps are required to obtain such highly accurate numerical solutions.

Table 4.12 Computed buckling load of column resting on elastic foundation with three end conditions compared with exact solution (P_{exact}) and benchmark numerical solution (P_{ref}) presented by Seemapholkul (2000). The number of adaptive steps is also indicated in the parenthesis

λ	K_1 (ksi)	K_2 (kips)	Pinned-pinned column		Fixed-pinned column		Fixed-fixed column	
			$P_{current}$ (ksi), (N)	P_{exact} (ksi)	$P_{current}$ (ksi), (N)	P_{ref} (ksi)	$P_{current}$ (ksi) , (N)	P_{ref} (ksi)
0	0	0	941.66 (4)	941.66	1,926 (5)	-	3,767 (4)	-
0	3	1000	16,856 (6)	16,856	17,797 (5)	17,800	20,443 (5)	20,448
2/3	0	0	938.19 (4)	938.19	1,911 (4)	-	3,712 (5)	-
2/3	0	0	20,504 (6)	20,504	20,801 (6)	-	22,810 (6)	-
2/3	3	1000	16,583 (5)	16,583	17,432 (5)	17,359	19,745 (5)	19,710
2/3	5	100	20,604 (6)	20,604	20,901 (6)	-	22,910 (6)	-

4.5 One story portal frame

Consider next a one-story portal frame with geometry, cross-sectional properties, loading conditions shown in Figure 4.7. The Young modulus and shear modulus of both beams and frames are given by E and G with Poisson ratio = 0.25. The

key objective here is to investigate the influence of the length ratio γ, the axial load ratio ρ, the moment of inertia ratios β and α, and the shear deformation of the column on values of the elastic buckling load. In the analysis, the reference stress σ_0 = 35143581 kg/m^2, the reference strain ε_0 = 0.00172405, I = 0.00013333 m^4, λ = 0.8331, A = 0.04 m^2 and L = 1 m are selected and the frame is discretized into three elements (one for beam and one for each column). A set of results for certain values of parameters {α, β, ρ, γ, μ} are reported in Table 4.10 for elastic buckling and in Table 4.11 and 4.12 for inelastic buckling and the corresponding buckling shapes for certain cases are also reported in Figure 4.8. To demonstrate the accuracy of the proposed technique, numerical results are compared with exact buckling loads (obtained by solving the differential equation and the corresponding exact eigenvalue problem) for columns without shear deformation and solutions obtained from a reliable FEM package for columns with shear deformation. As evident from computed results, the approximate buckling loads are in excellent agreement with the exact and benchmark solutions. In addition, the number of adaptive steps required to achieve the converged solutions for the elastic case are relatively few and much lower than that required for the inelastic case.
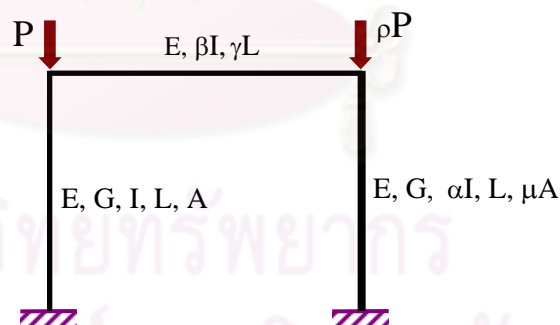

Figure 4.7 Schematic of axially-loaded, portal rigid frame

4.6 Multi-storey frame with side-sway restraint

As a final example, we consider a more complex problem associated with a multi-story rigid frame subjected to axial loads and braced against the lateral movement by elastic translational springs of stiffness k as depicted in Figure 4.9. The

Table 4.13 Normalized elastic buckling load ($P_{current}$) of one-story portal frame shown in Figure 4.4. Results are compared with exact solutions (P_{exact}) and benchmark solution (P_{FEM}) from FEM

α	β	ρ	γ	μ	No shear deformation		With column shear deformation	
					$\dfrac{P_{current}}{\pi^2 EI/L^2}$, (N)	$\dfrac{P_{exact}}{\pi^2 EI/L^2}$	$\dfrac{P_{current}}{\pi^2 EI/L^2}$, (N)	$\dfrac{P_{FEM}}{\pi^2 EI/L^2}$
1	1	1	1	1	0.747665 (3)	0.747665	0.696285 (4)	0.696506
5	1	1	1	1	1.434923 (4)	1.434923	1.229010 (5)	1.229351
1	5	1	1	1	0.936730 (4)	0.936730	0.857457 (3)	0.858177
1	1	5	1	1	0.247925 (4)	0.247925	0.229675 (4)	0.229879
1	1	1	5	1	0.443284 (3)	0.443284	0.424703 (4)	0.424821
1	1	1	1	5	0.747665 (3)	0.747665	0.716359 (3)	0.716851
5	1	0.1	1	1	2.553626 (4)	2.553626	2.115826 (6)	2.116454
1	1	0.1	1	5	1.348748 (4)	1.348748	1.283583 (4)	1.284468

Table 4.14 Normalized inelastic buckling load ($P_{current}$) of one-story portal frame shown in Figure 4.4. Results are compared with exact solutions (P_{exact})

α	β	ρ	γ	μ	No shear deformation			
					n =3, B = 2/3		n =4, B = ¾	
					$\dfrac{P_{current}}{\pi^2 EI/L^2}$, (N)	$\dfrac{P_{exact}}{\pi^2 EI/L^2}$	$\dfrac{P_{current}}{\pi^2 EI/L^2}$, (N)	$\dfrac{P_{FEM}}{\pi^2 EI/L^2}$
1	1	1	1	1	0.137838 (7)	0.137838	0.108516 (7)	0.108516
3	1	1	1	1	0.169497 (9)	0.169497	0.127253 (9)	0.127253
1	3	1	1	1	0.139310 (6)	0.139310	0.109194 (6)	0.109194
1	1	3	1	1	0.073092 (18)	0.073092	0.051308 (27)	0.051308
1	1	1	3	1	0.133370 (10)	0.133370	0.106430 (10)	0.106430
1	1	1	1	3	0.137838 (7)	0.137838	0.108516 (7)	0.108516
3	1	0.3	1	1	0.219724 (19)	0.219724	0.154005 (23)	0.154033
1	1	0.3	1	3	0.219412 (16)	0.219412	0.153920 (22)	0.153948

Table 4.14 (Cond.) Normalized inelastic buckling load ($P_{current}$) of one-story portal frame shown in Figure 4.4. Results are compared with exact solutions (P_{exact})

α	β	ρ	γ	μ	No shear deformation	
					n =5, B = 4/5	
					$\dfrac{P_{current}}{\pi^2 EI / L^2}$, (N)	$\dfrac{P_{exact}}{\pi^2 EI / L^2}$
1	1	1	1	1	0.093911 (7)	0.093911
3	1	1	1	1	0.106851 (9)	0.106851
1	3	1	1	1	0.094315 (6)	0.094315
1	1	3	1	1	0.041403 (35)	0.041415
1	1	1	3	1	0.092661 (9)	0.092661
1	1	1	1	3	0.093911 (7)	0.093911
3	1	0.3	1	1	0.124251 (13)	0.124294
1	1	0.3	1	3	0.124210 (32)	0.124261
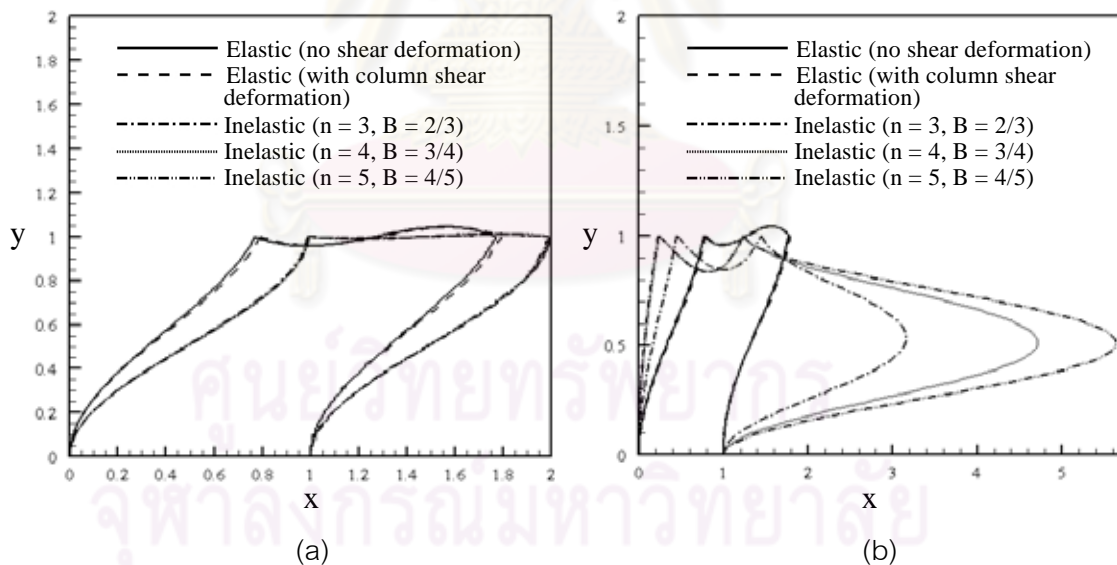
Figure 4.8 Buckling shapes of one story portal frame: (a) {α, β, ρ, γ, μ} = {1, 1, 1, 1, 1} and (b) {α, β, ρ, γ, μ} = {1, 1, 5, 1, 1} for elastic buckling and {α, β, ρ, γ, μ} = {1, 1, 3, 1, 1} for inelastic buckling

span length of each bay and the height of each levels are given by {2L, L, 2L} and {L, L, L, L, L}, respectively. The moment of inertia and the cross-sectional area of columns in

the first to fifth levels are given by {3I, 2I, 2I, I, I} and {3A, 2A, 2A, A, A}, respectively, whereas the moment of inertia and the cross-sectional area of all beams are given by I and A, respectively. The Young modulus and shear modulus of both beams and columns are given by E and G and the Poisson ratio is taken to be 0.25. In the analysis, the frame is discretized in to 35 members (20 elements for columns and 15 elements for beams) and I = 0.000675 m^4, λ = 0.8331, A = 0.09 m^2 and L = 1 m are employed. The normalized elastic buckling load of the frame, denoted by $\hat{P}_{current} = P_{current}/(\pi^2 EI/L^2)$, with and without shear deformation for various values of normalized spring stiffness, denoted by $\overline{k} = k/(\pi^2 EI/(2L)^3)$, are reported and compared with benchmark solutions obtained from a reliable FEM package in Figure 4.10. The buckling shapes of this frame are also reported in Figure 4.11 for certain values of $\overline{k}$. It is apparent that when the spring stiffness k reaches a certain finite value, the buckling load is identical to that of the same frame being fully fixed against the side-sway (i.e. k = ∞). Again, the switch of buckling modes can be accurately captured by the current technique. Note in addition that the shear deformation significantly lowers the flexural buckling load of this particular frame but insignificantly influences the buckling shape.
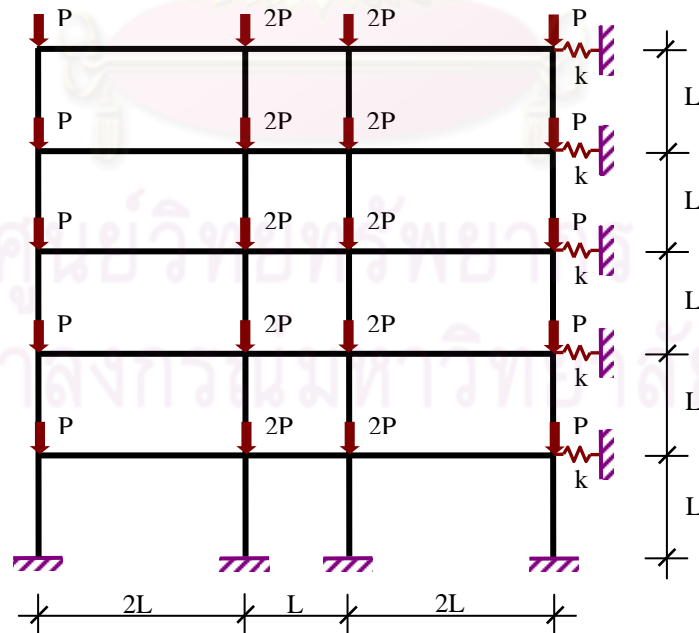

Figure 4.9 Schematic of axially-loaded, multi-story frame with side-sway restraints
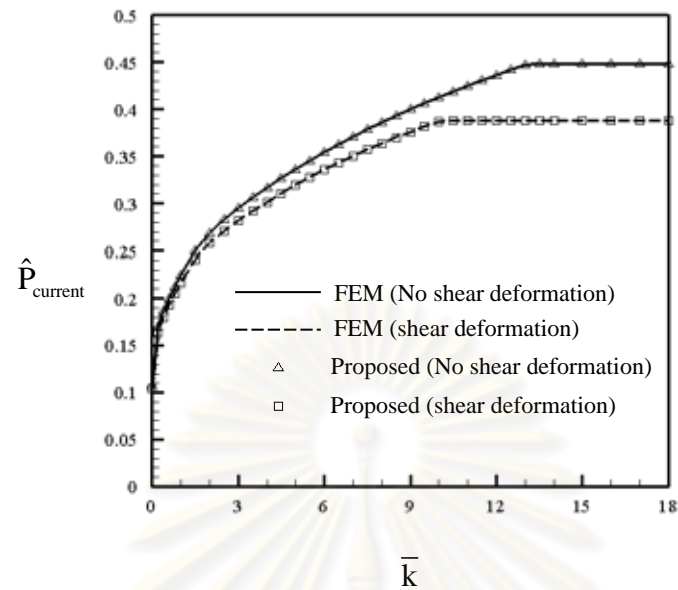
Figure 4.10 Normalized elastic buckling load of axially loaded, multi-story frame with side-sway restraints versus normalized spring stiffness
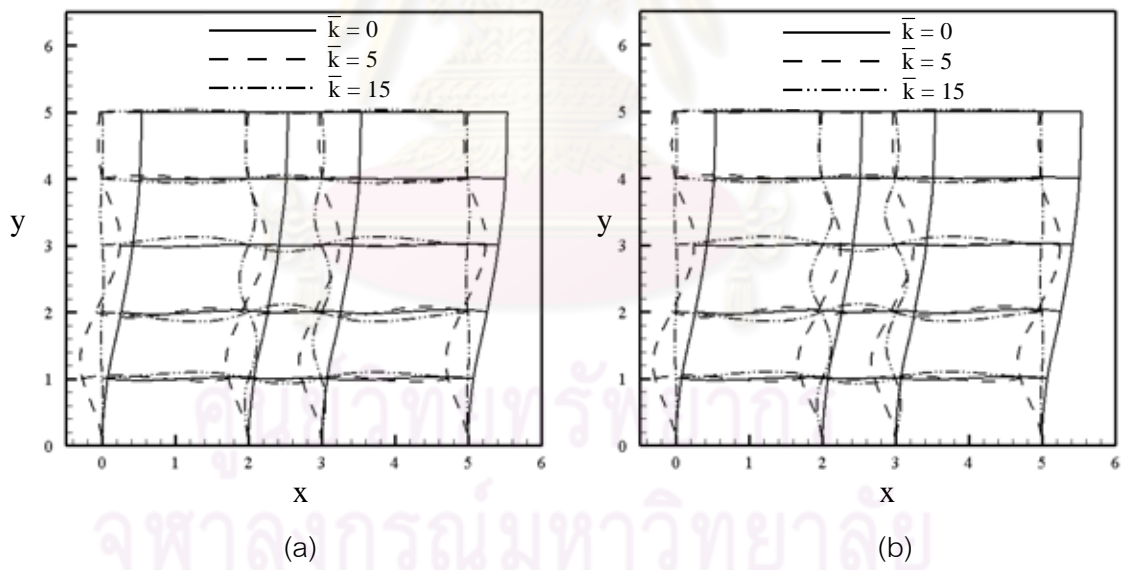

Figure 4.11 The buckling shapes of multi-storey frame with side-sway restraint: (a) without shear deformation and (b) with shear deformation

CHAPTER V

CONCLUSIONS AND REMARKS

An efficient and accurate numerical technique has been developed for estimating the flexural buckling load of two-dimensional, axially-loaded, skeleton structures with consideration of shear deformation, elastic lateral restraints and inelastic material behavior. The well-known principle of stationary total potential energy has been utilized to derive the variational formulation and the standard Rayleigh-Ritz approximation scheme has been adopted to construct a discretized eigenvalue problem. The capability of the proposed technique has been enhanced by supplying the automatic adaptivity to the finite element approximation via the successive improvement of the assumed buckling shape. The shape functions, used to form the trial functions for each element, have been derived from an exact function form of the buckling shape obtained directly by solving the differential equations. With such special development, the final shape functions possess two attractive features: (i) they contain an adaptive parameter involving the axial load of each element and (ii) they can represent an exact buckling shape of each element if the axial load is identical to the exact buckling load. A proper iterative procedure has been implemented along with the use of such special features of the shape functions to successively improve the buckling load estimation. The power method and the Rayleigh quotient technique have been used to determine the minimum eigenvalue and the corresponding eigenvector.

From extensive numerical experiments on various structures, it has been found that only a few adaptive steps to update the assumed buckling shapes are required to achieve the converged buckling load for a sufficiently small, specified tolerance. As compared with reliable benchmark solutions, the proposed technique has proven to yield highly accurate results comparable to exact solutions without any mesh refinement. In addition, by using the converged eigenvector obtained from the eigen-hunt in the previous step as an initial guess vector in the power method and Rayleigh quotient routine for computing the minimum eigenvalue, less number of iterations is required in the subsequent adaptive steps. In addition, the proposed technique can also

accurately predict the buckling load of structures that are braced against the lateral movement and may experience switch of the buckling modes.

A proposed computational procedure provides an attractive alternative to other available methods (e.g. analytical techniques, standard finite element method, etc.) for flexural buckling analysis of structures. Since it yields highly accurate numerical solutions comparable to the analytical solution for a broad class of structures, one direct application is to use this technique either to generate benchmark solutions for comparison purposes or as a computational tool for performing some parametric studies. Due to the automatic adaptivity embedded and no mesh refinement needed, meshing effort required for a large scale structure can be significantly reduced. Another application is to use this technique to correctly estimate the effective length factor of columns in both sway and non-sway multi-story frames. It has been found very often in various practical situations that alignment charts predict very inaccurate effective length factor. The accurate estimated effective length factor is essential in the design of members in compression and members in combined flexure and compression.

As a final remark, the proposed technique still possesses certain limitations and requires further investigations. For instance, it is not directly applicable to structures with members of varying cross sections, structures subjected to the distributed axial load, and structures with significant influence of the axial deformation. Also, structures consisting of members with singly-symmetric or non-symmetric cross section in which the flexural-torsional buckling is dominated cannot be treated.

REFERENCES

ACI Committee 318. 2005. <u>Building Code Requirements for Structural Concrete and Commentary</u>. American Concrete Institute.

Aristizabal-Ochoa, J.D. 1994. K-Factor for Column in Any Type of Construction: Non-Paradoxical Approach. <u>Journal of Structural Engineering</u> 120: 1273-1290.

Aristizabal-Ochoa, J.D. 1994. Slenderness K Factor for Leaning Columns. <u>Journal of Structural Engineering</u> 120: 2977-2991.

Blaauwendraad, J. 2008. Timoshenko Beam-Column Buckling. Does Dario Stand The Test?. <u>Engineering Structures</u> 30 : 3389-3393.

Considère, A. 1891. Resistance des pieces comprimèes. <u>Congrès International des Procèdés de Construction</u>. Paris.

Chajes, A. 1974. <u>Principle of Structural Stability Theory</u>. London: Prentice-Hall International.

Chapra, S.C., and Canale, R.P. 1990. <u>Numerical Methods for Engineers</u>. New York: McGraw-Hill.

Chen, W.F., and Lui, E.M. 1987. <u>Structural Stability: Theory and Implementation</u>. New York: Elsevier.

Cheng, F.Y., and Pantelides, C.P. 1988. Static Timoshenko Beam-Columns on Elastic Media. <u>Journal of Structural Engineering</u> 114(5): 1152-1172.

Choi, D.H., and Yoo, H. 2009. Iterative System Buckling Analysis, Considering a Fictitious Axial Force to Determine Effective Length Factors for Multi-Story Frames. <u>Engineering Structures</u> 31: 560-570.

Dawe, D.J. 1984. <u>Matrix and Finite Element Displacement Analysis of Structures</u>. New York: Oxford University Press.

Djukic, D. S., and Atanackovic, T.M. 1993. Effect of Shear on Simple Buckling Problem. <u>Journal of Engineering Mechanics</u> 119(5): 1108-1115.

Eisenberger, M., Yankelevsky. D.Z., and Clastornik, J. 1986. Stability of Beams on Elastic Foundation. <u>Computer & Structures</u> 24(1): 135-139.

Engesser, F. 1889. Ueber die Knickfestigkeit Gerader Stabe. <u>Zeitschrift des Architekten-und Ingenieur</u>. Vereins zu Hannover.

Engesser, F. 1891. Die Knickfestigkeit Gerader Stabe. <u>Zentralblatt der Bauverwaltung</u>. Berlin.

Gallagher, R.H., Ziemian, R.D., and McGuire, W. 2000. <u>Matrix Structural Analysis</u>. New Jersey: Courier Dover Publications.

Gantes, C.J., and Mageirou, G.E. 2005. Improved Stiffness Distribution Factors for Evaluation of Effective Buckling Lengths in Multi-Story Sway Frames. <u>Engineering Structures</u> 27: 1113-1124.

Gaylord, E.H., Gaylord, C.N., and Stallmeyer, J.E. 1992. <u>Design of Steel Structures</u>. 3rd ed. New York: McGraw-Hill.

Girgin, K., and Ozman, G. 2007. Simplified Procedure for Determining Buckling Loads of Three-Dimensional Framed Structures. <u>Engineering Structures</u> 29: 2344-2352.

Hamming, R. 1987. <u>Numerical Methods for Scientists and Engineers</u>. New York: Dover Publications.

Haringx, J.A. 1948. On Highly Compressible Helical Springs and Rubber Rods, and Their Application for Vibration-Free Mountings. <u>Philips research reports</u>: 1-97.

Hellesland, J., and Bjorhovde, R. 1996. Restraint Demand Factors and Effective Lengths of Braced Columns. <u>Journal of Structural Engineering</u> 122: 1216-1224.

Hellesland, J., and Bjorhovde, R. 1996. Improved Frame Stability Analysis With Effective Lengths. <u>Journal of Structural Engineering</u> 122: 1275-1283.

Hughes, T.J.R. 2000. <u>The Finite Element Method: Linear Static and Dynamic Finite Element Analysis</u>. New Jersey: Dover Publications.

Kassimali, A. 2005. <u>Structural Analysis</u>. 3rd ed. Victoria: Thomson.

Mahfouz, S.Y. 1999. <u>Design Optimization of Structural Steelwork</u>. Doctoral dissertation. Department of Civil and Environment Engineering, Faculty of University of Bradford(UK).

McCormac, J.C. 1994. <u>Structural Steel Design: LRFD Method</u>. 2nd ed. New York: Harper Collins Publishers.

Naidu, N.R., and Rao, G.V. 1995. Stability Behaviour of Uniform Column on a Class of Two-Parameter Elastic Foundation. <u>Computer & Structures</u> 57(3): 551-553.

Notay, Y. 2001. <u>Convergence Analysis of Inexact Rayleigh Quotient Iterations</u>. Tech. Rep. GANMN 01 02, Université Libre de Bruxelles, Brussels, Belgium.

Salmon, C.G., and Johnson, J.E. 1996. Steel Structures: Design and Behavior, Emphasizing Load and Resistance Factor Design. 4th ed. New York: HarperCollins College Publishers.

Seemapholkul, P. 2000. Buckling and Vibration Analysis of Timoshenko Beam-Column on Two-Parameter Elastic Foundation. Master's Thesis. Department of Civil Engineering. Faculty of King Mongkut's University of Technology Thonburi.

Shanley, F.R. 1946. The Column Paradox. Journal of the Aeronautical Sciences 13: 678

Specification for Structural Steel Buildings 2005. ANSI/AISC 360-05. American Institute of Steel Construction. Chicago.

Timoshenko, S.P. and Gere, J.M. 1961. Theory of Elastic Stability. 2nd ed. New York: McGraw-Hill.

Wang, C.M., Ng, K.H., and Kitipornchai, S. 2002. Stability Criteria for Timoshenko Columns with Intermediate and End Concentrated Axial Loads. Journal of Construction Steel Research 58(9): 1177-1193.

Xia, G.P., and Zhang, Z. 2009. A Numerical Method for Critical Buckling load for a Beam Supported on Elastic Foundation. EJGE 14.

Yang, T.Y. 1986. Finite Element Structural Analysis. New Jersey: Prentice-Hall.

Yankelevsky., D.Z., and Eisenberger, M. 1986. Analysis of a Beam Column on Elastic Foundation. Computer & Structures 23(3): 351-356.

Yoo, H., and Choi, D.H. 2008. New method of inelastic buckling analysis for steel frames. Journal of Constructional Steel Research 64(10): 1152-1164.

Zhohua, F., and Cook, R.D. 1983. Beam Element on Two-Parameter Elastic Foundation. Journal of Engineerig mechanics 109(6): 1390-1402.

Ziegler, H. 1982. Arguments for and Against Engesser's Buckling Formulas. Ingenieur-Archiv 52: 105-113.

APPENDICES

APPENDIX A

Constants a_m and Γ_{mi} appearing in equations (2.37) and (2.38) are given explicitly by

$$a_m = \left\{ \overline{\eta}_j \left(1 - \overline{\eta}_j \overline{P}_j + \overline{\eta}_j \overline{k}_{2j} \right) r_m^3 + \left(1 - \overline{\eta}_j^2 \overline{k}_{2j} \right) r_m \right\} \tag{A.1}$$

$$\Gamma_{11} = \left[(a_3 a_4 - a_2 a_4) e^{(r_2 + r_3)} + (a_2 a_3 - a_3 a_4) e^{(r_2 + r_4)} - a_2 a_3 + a_2 a_4 \right] / \Omega \tag{A.2}$$

$$\Gamma_{21} = \left[(a_1 a_4 - a_3 a_4) e^{(r_1 + r_3)} + (a_3 a_4 - a_1 a_3) e^{(r_1 + r_4)} + a_1 a_3 - a_1 a_4 \right] / \Omega \tag{A.3}$$

$$\Gamma_{31} = \left[(a_2 a_4 - a_1 a_4) + (a_1 a_2 - a_2 a_4) e^{(r_1 + r_4)} + (a_1 a_4 - a_1 a_2) e^{(r_2 + r_4)} \right] / \Omega \tag{A.4}$$

$$\Gamma_{41} = \left[(a_1 a_3 - a_2 a_3) + (a_2 a_3 - a_1 a_2) e^{(r_1 + r_3)} + (a_1 a_2 - a_1 a_3) e^{(r_2 + r_3)} \right] / \Omega \tag{A.5}$$

$$\Gamma_{12} = \left[(a_2 - a_3) e^{(r_2 + r_3)} + (a_4 - a_2) e^{(r_2 + r_4)} + a_3 - a_4 \right] / \Omega \tag{A.6}$$

$$\Gamma_{22} = \left[(a_3 - a_1) e^{(r_1 + r_3)} + (a_1 - a_4) e^{(r_1 + r_4)} - a_3 + a_4 \right] / \Omega \tag{A.7}$$

$$\Gamma_{32} = \left[(a_1 - a_2) + (a_4 - a_1) e^{(r_1 + r_4)} + (a_2 - a_4) e^{(r_2 + r_4)} \right] / \Omega \tag{A.8}$$

$$\Gamma_{42} = \left[(a_2 - a_1) + (a_1 - a_3) e^{(r_1 + r_3)} + (a_3 - a_2) e^{(r_2 + r_3)} \right] / \Omega \tag{A.9}$$

$$\Gamma_{13} = \left[(a_2 a_4 - a_2 a_3) e^{r_2} + (a_2 a_3 - a_3 a_4) e^{r_3} + (a_3 a_4 - a_2 a_4) e^{r_4} \right] / \Omega \tag{A.10}$$

$$\Gamma_{23} = \left[(a_1 a_3 - a_1 a_4) e^{r_1} + (a_3 a_4 - a_1 a_3) e^{r_3} + (a_1 a_4 - a_3 a_4) e^{r_4} \right] / \Omega \tag{A.11}$$

$$\Gamma_{33} = \left[(a_1 a_4 - a_1 a_2) e^{r_1} + (a_1 a_2 - a_2 a_4) e^{r_2} + (a_2 a_4 - a_1 a_4) e^{r_4} \right] / \Omega \tag{A.12}$$

$$\Gamma_{43} = \left[(a_1 a_2 - a_1 a_3) e^{r_1} + (a_2 a_3 - a_1 a_2) e^{r_2} + (a_1 a_3 - a_2 a_3) e^{r_3} \right] / \Omega \tag{A.13}$$

$$\Gamma_{14} = \left[(a_3 - a_4) e^{r_2} + (a_4 - a_2) e^{r_3} + (a_2 - a_3) e^{r_4} \right] / \Omega \tag{A.14}$$

$$\Gamma_{24} = \left[(a_4 - a_3) e^{r_1} + (a_1 - a_4) e^{r_3} + (a_3 - a_1) e^{r_4} \right] / \Omega \tag{A.15}$$

$$\Gamma_{34} = \left[(a_2 - a_4) e^{r_1} + (a_4 - a_1) e^{r_2} + (a_1 - a_2) e^{r_4} \right] / \Omega \tag{A.16}$$

$$\Gamma_{44} = \left[(a_3 - a_2) e^{r_1} + (a_1 - a_3) e^{r_2} + (a_2 - a_1) e^{r_3} \right] / \Omega \tag{A.17}$$

$$\begin{aligned} \Omega = &\, 2 \left(a_1 a_3 - a_1 a_4 - a_2 a_3 + a_2 a_4 \right) + \left(-a_1 a_2 + a_1 a_4 + a_2 a_3 - a_3 a_4 \right) \left[e^{(r_1 + r_3)} + e^{(r_2 + r_4)} \right] \\ &+ \left(a_1 a_2 - a_1 a_3 - a_2 a_4 + a_3 a_4 \right) \left[e^{(r_1 + r_4)} + e^{(r_2 + r_3)} \right] \end{aligned} \tag{A.18}$$

APPENDIX B

The shape functions $\psi_i(\overline{x})$ and $\widehat{\psi}_i(\overline{x})$ for a special case without the elastic lateral restraint (i.e. $k_{1i}=0$ and $k_{2i}=0$). The governing differential equation (2.27) simply reduces to

$$r^4 + 2\overline{\varpi}r^2 = 0 \tag{B.1}$$

where

$$\overline{\varpi} = \frac{\overline{P}_j}{2\left(1 - \overline{\eta}_j\overline{P}_j\right)} \tag{B.2}$$

The general solution of buckling shape $\overline{v}(\overline{x})$ and $\beta(\overline{x})$ takes the form

$$\overline{v}(\overline{x}) = C_1 e^{r_1\overline{x}} + C_2 e^{r_2\overline{x}} + C_3\overline{x} + C_4 \tag{B.3}$$

$$\beta(\overline{x}) = \tilde{C}_1 e^{r_1\overline{x}} + \tilde{C}_2 e^{r_2\overline{x}} + C_3 \tag{B.4}$$

where C_1, C_2, C_3 and C_4 are arbitrary constants, r_1 and r_2 are distinct roots of the characteristic equation (B.1), and

$$\tilde{C}_m = \left\{\overline{\eta}_j\left(1 - \overline{\eta}_j\overline{P}_j\right)r_m^3 + r_m\right\}C_m \tag{B.5}$$

By enforcing essential boundary conditions (2.34) along with using the relation (B.5), it leads to the same form of buckling shapes as that shown in equation (2.35) - (2.36) but the shape functions $\psi_i(x)$ and $\widehat{\psi}_i(x)$ are given differently by

$$\psi_i(\overline{x}) = \sum_{m=1}^{2}\Gamma_{mi}e^{r_m\overline{x}} + \Gamma_{3i}\overline{x} + \Gamma_{4i} \tag{B.6}$$

$$\widehat{\psi}_i(\overline{x}) = \sum_{m=1}^{2}a_m\Gamma_{mi}e^{r_m\overline{x}} + \Gamma_{3i} \tag{B.7}$$

where constants a_m and Γ_{mi} are given explicitly by

$$\tilde{a}_m = \left\{\overline{\eta}_j\left(1 - \overline{\eta}_j\overline{P}_j\right)r_m^3 + r_m\right\} \tag{B.8}$$

$$\Gamma_{11} = \left[\tilde{a}_2(1 - e^{r_2})\right]\Big/\Omega \tag{B.9}$$

$$\Gamma_{21} = \left[\tilde{a}_1(e^{r_1} - 1) \right] \big/ \Omega \tag{B.10}$$

$$\Gamma_{31} = \left[\tilde{a}_1 \tilde{a}_2(e^{r_2} - e^{r_1}) \right] \big/ \Omega \tag{B.11}$$

$$\Gamma_{41} = \left[(\tilde{a}_1 \tilde{a}_2 - \tilde{a}_2)e^{r_1} + (\tilde{a}_1 - \tilde{a}_1 \tilde{a}_2)e^{r_2} + \tilde{a}_2 - \tilde{a}_1 \right] \big/ \Omega \tag{B.12}$$

$$\Gamma_{12} = \left[(1 - \tilde{a}_2)e^{r_2} - 1 \right] \big/ \Omega \tag{B.13}$$

$$\Gamma_{22} = \left[1 + (\tilde{a}_1 - 1)e^{r_1} \right] \big/ \Omega \tag{B.14}$$

$$\Gamma_{32} = \left[\tilde{a}_1 e^{r_1} - \tilde{a}_2 e^{r_2} + \tilde{a}_2 - \tilde{a}_1 \right] \big/ \Omega \tag{B.15}$$

$$\Gamma_{42} = \left[(1 - \tilde{a}_1)e^{r_1} + (\tilde{a}_2 - 1)e^{r_2} \right] \big/ \Omega \tag{B.16}$$

$$\Gamma_{13} = \left[\tilde{a}_2(e^{r_2} - 1) \right] \big/ \Omega \tag{B.17}$$

$$\Gamma_{23} = \left[\tilde{a}_1(1 - e^{r_1}) \right] \big/ \Omega \tag{B.18}$$

$$\Gamma_{33} = \left[\tilde{a}_1 \tilde{a}_2(e^{r_1} - e^{r_2}) \right] \big/ \Omega \tag{B.19}$$

$$\Gamma_{43} = \left[\tilde{a}_1(e^{r_1} - 1) + \tilde{a}_2(1 - e^{r_2}) \right] \big/ \Omega \tag{B.20}$$

$$\Gamma_{14} = \left[1 + \tilde{a}_2 - e^{r_2} \right] \big/ \Omega \tag{B.21}$$

$$\Gamma_{24} = \left[e^{r_1} - \tilde{a}_1 - 1 \right] \big/ \Omega \tag{B.22}$$

$$\Gamma_{34} = \left[\tilde{a}_2(1 - e^{r_1}) + \tilde{a}_1(e^{r_2} - 1) \right] \big/ \Omega \tag{B.23}$$

$$\Gamma_{44} = \left[\tilde{a}_1 - \tilde{a}_2 - e^{r_1} + e^{r_2} \right] \big/ \Omega \tag{B.24}$$

$$\Omega = 2(\tilde{a}_2 - \tilde{a}_1) + (\tilde{a}_1 + \tilde{a}_2)\left[e^{r_1} + e^{r_2} \right] + \tilde{a}_1 \tilde{a}_2 \left[e^{r_1} - e^{r_2} \right] \tag{B.25}$$

Since the shape function $\psi_i(\overline{x})$ and $\hat{\psi}_i(\overline{x})$ are given in terms of exponential and linear functions, all elements stiffness matrices $\mathbf{K}_{bi}$, $\mathbf{K}_{si}$, and $\mathbf{K}_{gi}$ can readily be obtained in an explicit form via the direct integration. Entries of these matrices are given by

$$\left[K_{bi} \right]_{mn} = E_i I_i \sum_{j=1}^{2} \sum_{k=1}^{2} \tilde{a}_j \tilde{a}_k r_j r_k \Gamma_{jm} \Gamma_{kn} \left(e^{(r_j + r_k)L} - 1 \right) \big/ \left(r_j + r_k \right) \tag{B.26}$$

$$\left[K_{si} \right]_{mn} = \lambda_i G_i A_i \sum_{j=1}^{2} \sum_{k=1}^{2} (r_j - \tilde{a}_j)(r_k - \tilde{a}_k) \Gamma_{jm} \Gamma_{kn} \left(e^{(r_j + r_k)L} - 1 \right) \big/ \left(r_j + r_k \right) \tag{B.27}$$

$$\left[K_{gi} \right]_{mn} = P_i \sum_{j=1}^{2} \sum_{k=1}^{2} r_j r_k \Gamma_{jm} \Gamma_{kn} \left(e^{(r_j + r_k)L} - 1 \right) \Big/ \left(r_j + r_k \right) + \sum_{j=1}^{2} \Gamma_{jm} \Gamma_{3n} \left(e^{r_j L} - 1 \right)$$

$$+ \sum_{k=1}^{2} \Gamma_{kn} \Gamma_{3m} \left(e^{r_k L} - 1 \right) + \Gamma_{3m} \Gamma_{3n}$$

(B.28)

APPENDIX C

The shape functions $\psi_i(\overline{x})$ and $\hat{\psi}_i(\overline{x})$ for a special case without the elastic lateral restraint (i.e. $k_{1i}=0$ and $k_{2i}=0$) and shear deformation. The governing differential equation (2.27) simply reduces to

$$\frac{d^4v}{dx^4}+k^2\frac{d^2v}{dx^2}=0 \tag{C.1}$$

where

$$k=\sqrt{\frac{P}{EI}} \tag{C.2}$$

The general solution of buckling shape $\overline{v}(\overline{x})$ takes the form

$$\overline{v}(\overline{x})=C_1+C_2\overline{x}+C_3\cos(\gamma\overline{x})+C_4\sin(\gamma\overline{x}) \tag{C.3}$$

where C_1, C_2, C_3 and C_4 are arbitrary constant and $\gamma=kL$. By enforcing essential boundary conditions (2.34), it leads to the same form of buckling shapes as that shown in equation (2.35) but the shape functions $\psi_i(x)$ are given differently by

$$\psi_1(\overline{x})=\frac{1}{\Gamma_2+2\Gamma_1}\left\{\Gamma_1+\Gamma_2-\Gamma_2\overline{x}+\Gamma_1\cos(\gamma\overline{x})+\Gamma_3\sin(\gamma\overline{x})\right\} \tag{C.4}$$

$$\psi_2(\overline{x})=\frac{1}{\gamma\left(\Gamma_2+2\Gamma_1\right)}\left\{\Gamma_4+\Gamma_1\gamma\overline{x}-\Gamma_4\cos(\gamma\overline{x})+(\Gamma_1+\Gamma_2)\sin(\gamma\overline{x})\right\} \tag{C.5}$$

$$\psi_3(\overline{x})=\frac{1}{\Gamma_2+2\Gamma_1}\left\{\Gamma_1+\Gamma_2\overline{x}-\Gamma_1\cos(\gamma\overline{x})-\Gamma_3\sin(\gamma\overline{x})\right\} \tag{C.6}$$

$$\psi_4(\overline{x})=\frac{1}{\gamma\left(\Gamma_2+2\Gamma_1\right)}\left\{\Gamma_5+\Gamma_1\gamma\overline{x}-\Gamma_5\cos(\gamma\overline{x})-\Gamma_1\sin(\gamma\overline{x})\right\} \tag{C.7}$$

where $\Gamma_1=\cos\gamma-1$, $\Gamma_2=\gamma\sin\gamma$, $\Gamma_3=\sin\gamma$, $\Gamma_4=\sin\gamma-\gamma\cos\gamma$ and $\Gamma_5=\gamma-\sin\gamma$. Note that the buckling shape $\beta(\overline{x})$ can be obtained by taking derivative of (2.35) with respect to $\overline{x}$. Since the shape function $\psi_i(\overline{x})$ are given in terms of trigonometric and linear functions, all elements stiffness matrices $\mathbf{K}_{bi}$ and $\mathbf{K}_{gi}$ can readily be obtained in an explicit form via the direct integration. Entries of these matrices are given by

$$[K_b]_{11} = \frac{\gamma^3 \left[2\Gamma_1\Gamma_3(1-\cos^2\gamma)+\cos\gamma\sin\gamma(\Gamma_1^2-\Gamma_3^2)+\beta(\Gamma_1^2+\Gamma_3^2) \right]}{2(\Gamma_2+2\Gamma_1)^2} \tag{C.8}$$

$$[K_b]_{12} = \frac{\gamma^2 \left[(1-\cos^2\gamma)(\Gamma_1^2+\Gamma_1\Gamma_2)+(\cos^2\gamma-1)\Gamma_3\Gamma_4-\cos\gamma\sin\gamma(\Gamma_1\Gamma_3+\Gamma_1\Gamma_4+\Gamma_2\Gamma_3) \right]}{2(\Gamma_2+2\Gamma_1)^2}$$
$$+ \frac{\gamma^2 \left[\gamma(\Gamma_1\Gamma_3-\Gamma_1\Gamma_4+\Gamma_2\Gamma_3) \right]}{2(\Gamma_2+2\Gamma_1)^2} \tag{C.9}$$

$$[K_b]_{13} = -[K_b]_{11} \tag{C.10}$$

$$[K_b]_{14} = \frac{\gamma^2 \left[(\cos^2\gamma-1)(\Gamma_1^2+\Gamma_3\Gamma_5)+\Gamma_1\cos\gamma\sin\gamma(\Gamma_3-\Gamma_5)-\gamma\Gamma_1(\Gamma_3+\Gamma_5) \right]}{2(\Gamma_2+2\Gamma_1)^2} \tag{C.11}$$

$$[K_b]_{22} = \frac{\gamma \left[2\Gamma_4(\cos^2\gamma-1)(\Gamma_1+\Gamma_2)-\cos\gamma\sin\gamma(\Gamma_1^2+2\Gamma_1\Gamma_2+\Gamma_2^2-\Gamma_4^2) \right]}{2(\Gamma_2+2\Gamma_1)^2}$$
$$+ \frac{\gamma \left[\gamma(\Gamma_1^2+2\Gamma_1\Gamma_2+\Gamma_2^2+\Gamma_4^2) \right]}{2(\Gamma_2+2\Gamma_1)^2} \tag{C.12}$$

$$[K_b]_{23} = -[K_b]_{12} \tag{C.13}$$

$$[K_b]_{24} = \frac{\gamma \left[(1-\cos^2\gamma)\Gamma_1\Gamma_4+(\cos^2\gamma-1)(\Gamma_1\Gamma_5+\Gamma_2\Gamma_5)-\gamma(\Gamma_1^2+\Gamma_1\Gamma_2-\Gamma_4\Gamma_5) \right]}{2(\Gamma_2+2\Gamma_1)^2}$$
$$+ \frac{\gamma \left[\cos\gamma\sin\gamma(\Gamma_1^2+\Gamma_1\Gamma_2+\Gamma_4\Gamma_5) \right]}{2(\Gamma_2+2\Gamma_1)^2} \tag{C.14}$$

$$[K_b]_{33} = [K_b]_{11} \tag{C.15}$$

$$[K_b]_{34} = -[K_b]_{14} \tag{C.16}$$

$$[K_b]_{44} = \frac{\gamma \left[2\Gamma_1\Gamma_5(1-\cos^2\gamma)+\cos\gamma\sin\gamma(\Gamma_5^2-\Gamma_1^2)+\gamma(\Gamma_1^2+\Gamma_5^2) \right]}{2(\Gamma_2+2\Gamma_1)^2} \tag{C.17}$$

$$[K_g]_{11} = \frac{2\gamma\Gamma_1\Gamma_3(\cos^2\gamma-1)+\gamma\cos\gamma\sin\gamma(\Gamma_3^2-\Gamma_1^2)+\gamma^2(\Gamma_1^2+\Gamma_3^2)}{2(\Gamma_2+2\Gamma_1)^2}$$
$$+ \frac{2(\Gamma_2^2+2\Gamma_1\Gamma_2(1-\cos\gamma)-2\Gamma_2\Gamma_3\sin\gamma)}{2(\Gamma_2+2\Gamma_1)^2} \tag{C.18}$$

$$[K_g]_{12} = \frac{\gamma \left[(\cos^2\gamma-3)(\Gamma_1^2+\Gamma_1\Gamma_2)+(1-\cos^2\gamma)\Gamma_3\Gamma_4 \right]+2\cos\gamma(\Gamma_2\Gamma_4+\gamma\Gamma_1^2)}{2\gamma(\Gamma_2+2\Gamma_1)^2}$$
$$+ \frac{\gamma\cos\gamma\sin\gamma(\Gamma_1\Gamma_3+\Gamma_1\Gamma_4+\Gamma_2\Gamma_3)-2\sin\gamma(\Gamma_1\Gamma_2+\Gamma_2^2-\gamma\Gamma_1\Gamma_3)-2\Gamma_2\Gamma_4}{2\gamma(\Gamma_2+2\Gamma_1)^2}$$
$$+ \frac{\gamma^2(\Gamma_1\Gamma_3-\Gamma_1\Gamma_4+\Gamma_2\Gamma_3)}{2\gamma(\Gamma_2+2\Gamma_1)^2} \tag{C.19}$$

$$\left[K_g\right]_{13} = -\left[K_g\right]_{11} \tag{C.20}$$

$$\left[K_g\right]_{14} = \frac{-\gamma\left[(1+\cos^2\gamma)\Gamma_1^{\,2}+(\cos^2\gamma-1)\Gamma_3\Gamma_5\right]-\gamma^2(\Gamma_1\Gamma_3+\Gamma_1\Gamma_5)-2\Gamma_2(\Gamma_5+\gamma\Gamma_1)}{2\gamma(\Gamma_2+2\Gamma_1)^2}$$
$$+\frac{\gamma\cos\gamma\sin\gamma(\Gamma_1\Gamma_5-\Gamma_1\Gamma_3)+2\cos\gamma(\Gamma_2\Gamma_5+\gamma\Gamma_1^{\,2})+2\Gamma_1\sin\gamma(\Gamma_2+\gamma\Gamma_3)}{2\gamma(\Gamma_2+2\Gamma_1)^2} \tag{C.21}$$

$$\left[K_g\right]_{22} = \frac{2\left[(3-\cos^2\gamma)\Gamma_1\Gamma_4+(1-\cos^2\gamma)\Gamma_2\Gamma_4\right]+\cos\gamma\sin\gamma(\Gamma_1^{\,2}+2\Gamma_1\Gamma_2+\Gamma_2^{\,2}-\Gamma_4^{\,2})}{2\gamma(\Gamma_2+2\Gamma_1)^2}$$
$$+\frac{\gamma(3\Gamma_1^{\,2}+2\Gamma_1\Gamma_2+\Gamma_2^{\,2}+\Gamma_4^{\,2})-4\Gamma_1\Gamma_4\cos\gamma+4\sin\gamma(\Gamma_1^{\,2}+\Gamma_1\Gamma_2)}{2\gamma(\Gamma_2+2\Gamma_1)^2} \tag{C.22}$$

$$\left[K_g\right]_{23} = -\left[K_g\right]_{12} \tag{C.23}$$

$$\left[K_g\right]_{24} = \frac{\left[(1+\cos^2\gamma)\Gamma_1\Gamma_4+(3-\cos^2\gamma)\Gamma_1\Gamma_5+(1-\cos^2\gamma)\Gamma_2\Gamma_5\right]-2\Gamma_1\cos\gamma(\Gamma_4+\Gamma_5)}{2\gamma(\Gamma_2+2\Gamma_1)^2}$$
$$+\frac{\gamma(\Gamma_1^{\,2}-\Gamma_1\Gamma_2+\Gamma_4\Gamma_5)-\cos\gamma\sin\gamma(\Gamma_1^{\,2}+\Gamma_1\Gamma_2+\Gamma_4\Gamma_5)+2\Gamma_1\Gamma_2\sin\gamma}{2\gamma(\Gamma_2+2\Gamma_1)^2} \tag{C.24}$$

$$\left[K_g\right]_{33} = \left[K_g\right]_{11} \tag{C.25}$$

$$\left[K_g\right]_{34} = -\left[K_g\right]_{14} \tag{C.26}$$

$$\left[K_g\right]_{44} = \frac{2\Gamma_1\Gamma_5(1+\cos^2\gamma)+\cos\gamma\sin\gamma(\Gamma_1^{\,2}-\Gamma_5^{\,2})+\gamma(3\Gamma_1^{\,2}+\Gamma_5^{\,2})-4\Gamma_1\Gamma_5\cos\gamma-4\Gamma_1^{\,2}\sin\gamma}{2\gamma(\Gamma_2+2\Gamma_1)^2} \tag{C.27}$$

ศูนย์วิทยทรัพยากร
จุฬาลงกรณ์มหาวิทยาลัย

BIOGRAPHY

Mr. Nidvichai Watcharakorn was born in 1987, at Ramathibodi Hospital, Bangkok. He graduated from Suankularb Wittayalai School in 2004, and enrolled in B.Eng. and M. Eng. courses at Department of Civil Engineering Faculty, Chulalongkorn University. The major in his master's degree is structural civil engineering, which includes studies and researches in structural mechanics and with advanced mathematical techniques. This thesis aims to investigate the flexural buckling load of structures.